Radial Basis Functions for Computational Geosciences*

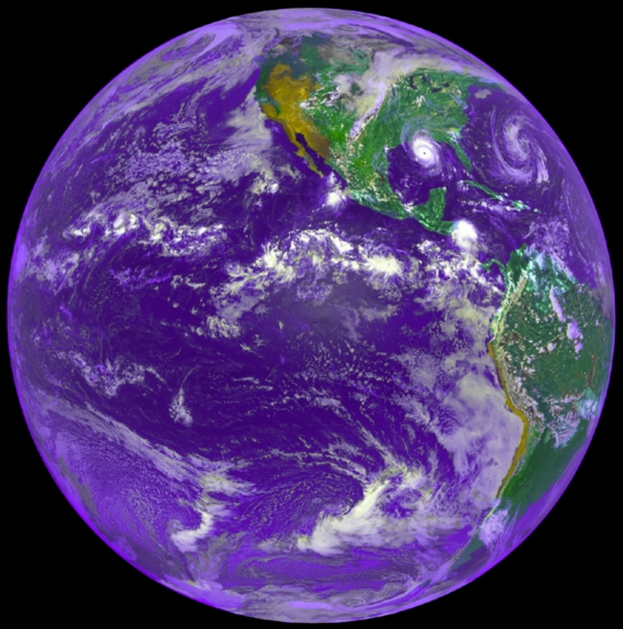

Grady B. Wright
Department of Mathematics
Boise State University

Natasha Flyer
Institute for Mathematics Applied to Geosciences
National Center for Atmospheric Research

*This work is supported by NSF CMG grants ATM 0801309 and DMS 0934581

Overview of this tutorial

Topics to cover:

- Brief introduction to interpolation with Radial Basis Functions (RBFs).
- Shallow water wave equations on a rotating sphere.
- Thermal convection in a 3D spherical shell: mantle convection.
- Reconstruction and decomposition of geophysically relevant vector fields.

Introduction to RBFs via interpolation

Key idea: linear combination of translates and rotations of a single radial function:

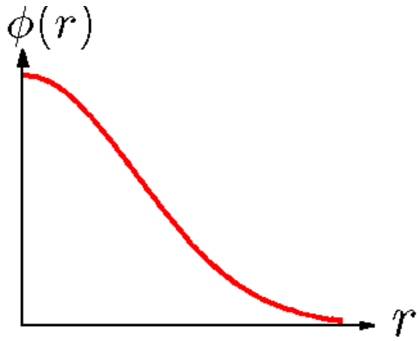

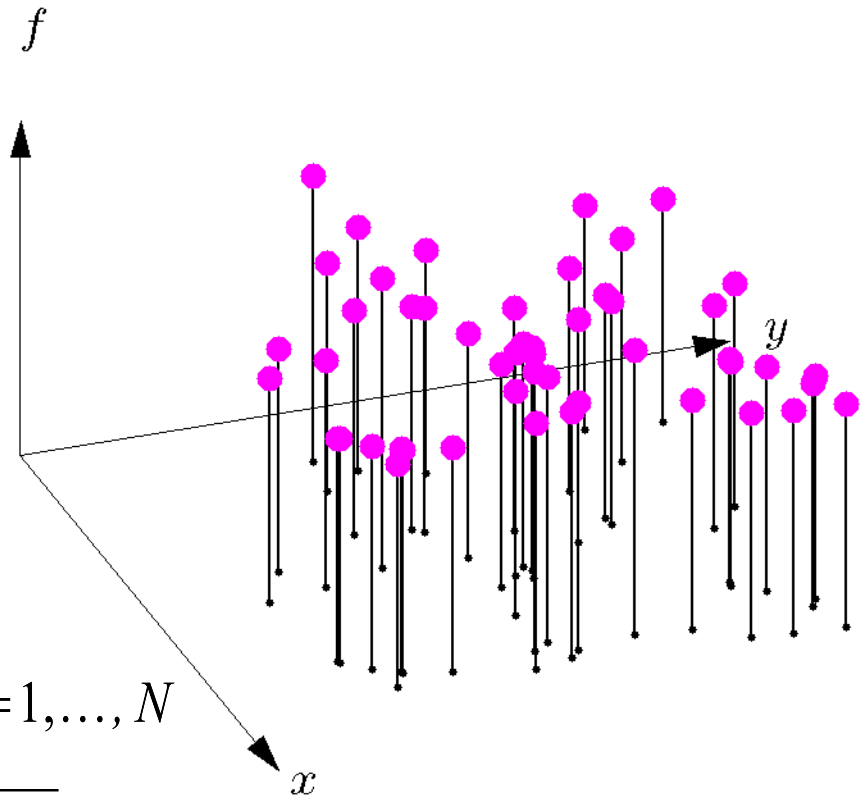

Interpolant:

$$s(\boldsymbol{x}) = \sum_{j=1}^{N} \beta_j \phi(\epsilon \|\boldsymbol{x} - \boldsymbol{x}_j\|), \quad s(\boldsymbol{x}_k) = f_k, \; k = 1, \ldots, N$$

where $\|\boldsymbol{x} - \boldsymbol{x}_j\| = \sqrt{(x - x_j)^2 + (y - y_j)^2}$

Introduction to RBFs via interpolation

Key idea: linear combination of translates and rotations of a single radial function:

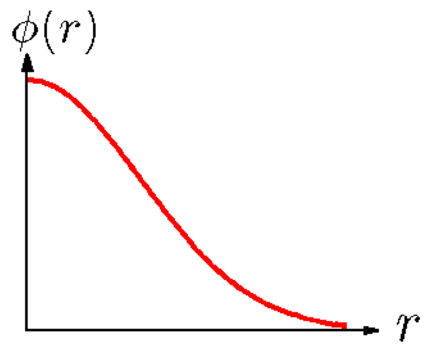

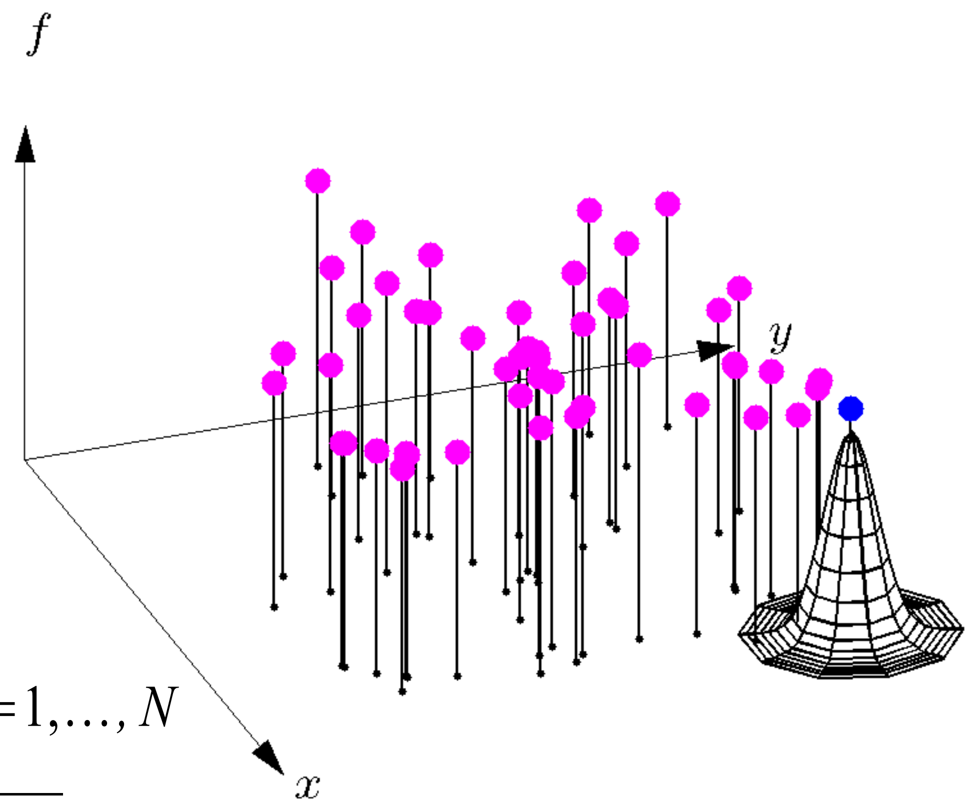

Interpolant:

$$s(\boldsymbol{x})=\sum_{j=1}^{N}\beta_j\phi(\epsilon\|\boldsymbol{x}-\boldsymbol{x}_j\|),\quad s(\boldsymbol{x}_k)=f_k,\ k=1,\ldots,N$$

where $\|\boldsymbol{x}-\boldsymbol{x}_j\|=\sqrt{(x-x_j)^2+(y-y_j)^2}$

Introduction to RBFs via interpolation

Key idea: linear combination of translates and rotations of a single radial function:

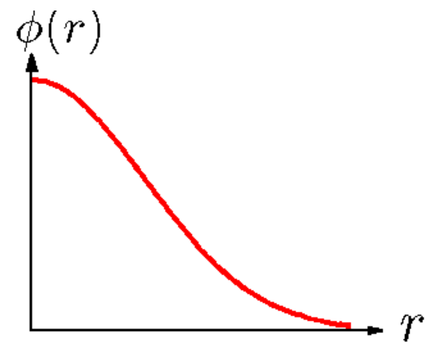

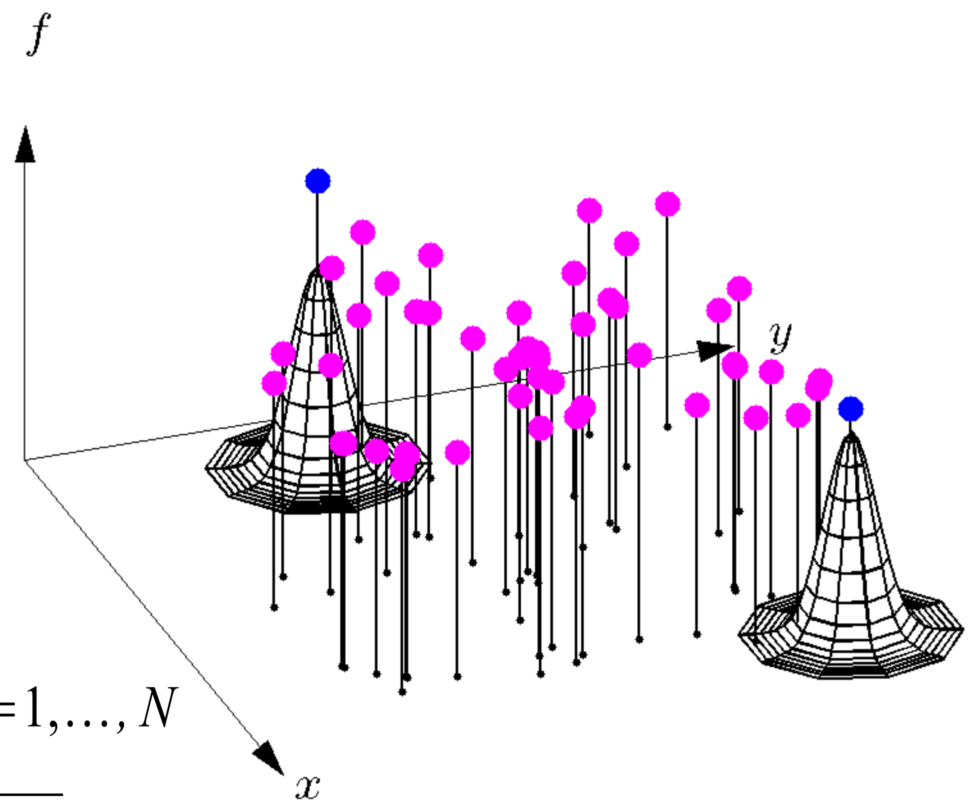

Interpolant:

$$s(\boldsymbol{x})=\sum_{j=1}^{N}\beta_j\,\phi(\epsilon\|\boldsymbol{x}-\boldsymbol{x}_j\|),\quad s(\boldsymbol{x}_k)=f_k,\ k=1,\ldots,N$$

where $\|\boldsymbol{x}-\boldsymbol{x}_j\|=\sqrt{(x-x_j)^2+(y-y_j)^2}$

Introduction to RBFs via interpolation

Key idea: linear combination of translates and rotations of a single radial function:

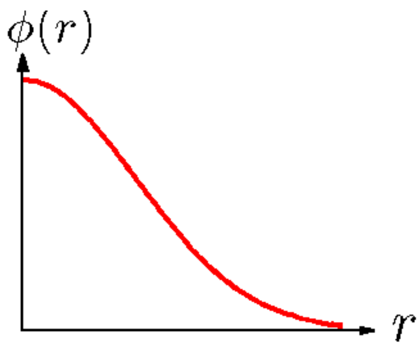

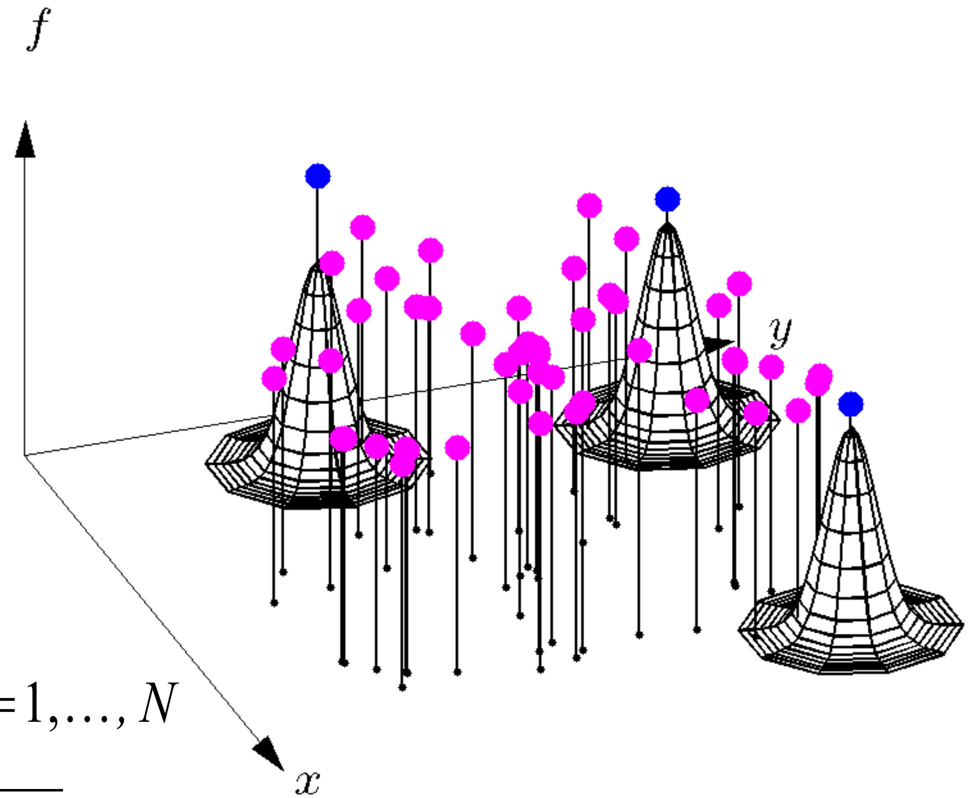

Interpolant:

$$s(\boldsymbol{x}) = \sum_{j=1}^{N} \beta_j \phi(\epsilon \| \boldsymbol{x} - \boldsymbol{x}_j \|), \quad s(\boldsymbol{x}_k) = f_k,\ k = 1, \ldots, N$$

where $\quad \| \boldsymbol{x} - \boldsymbol{x}_j \| = \sqrt{(x - x_j)^2 + (y - y_j)^2}$

Introduction to RBFs via interpolation

Key idea: linear combination of translates and rotations of a single radial function:

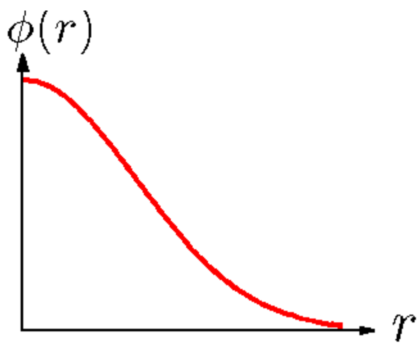

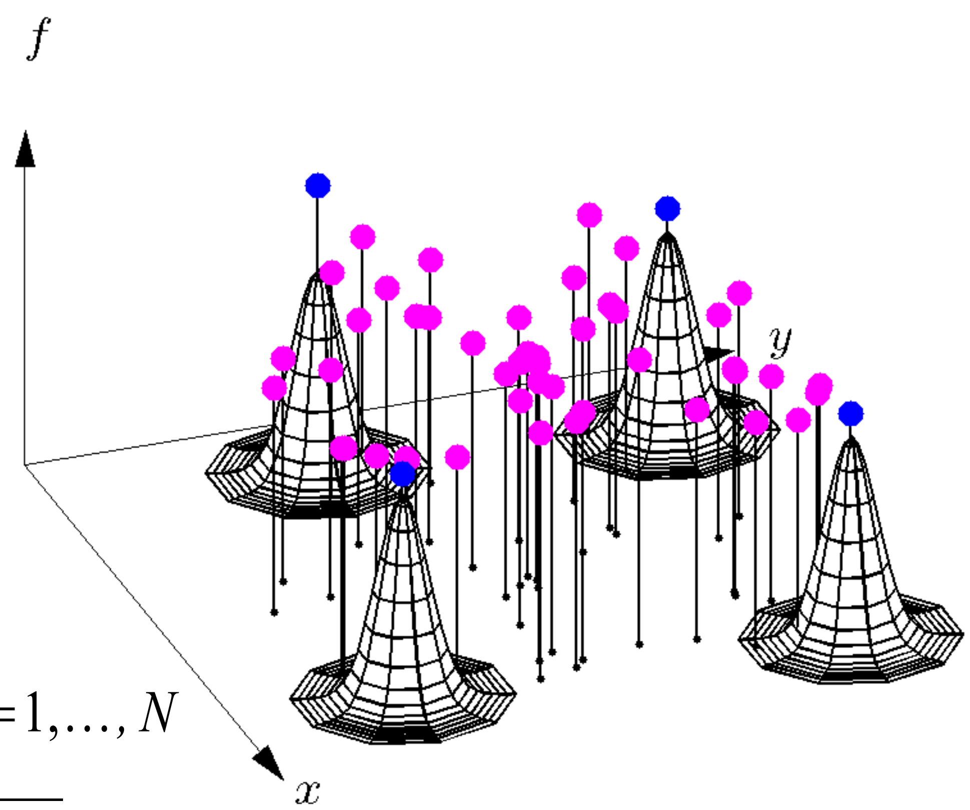

Interpolant:

$$s(\boldsymbol{x}) = \sum_{j=1}^{N} \beta_j \phi(\epsilon \| \boldsymbol{x} - \boldsymbol{x}_j \|), \quad s(\boldsymbol{x}_k) = f_k, \; k = 1, \ldots, N$$

where $\quad \| \boldsymbol{x} - \boldsymbol{x}_j \| = \sqrt{(x - x_j)^2 + (y - y_j)^2}$

Introduction to RBFs via interpolation

Key idea: linear combination of translates and rotations of a single radial function:

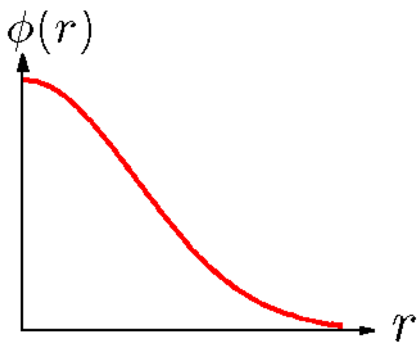

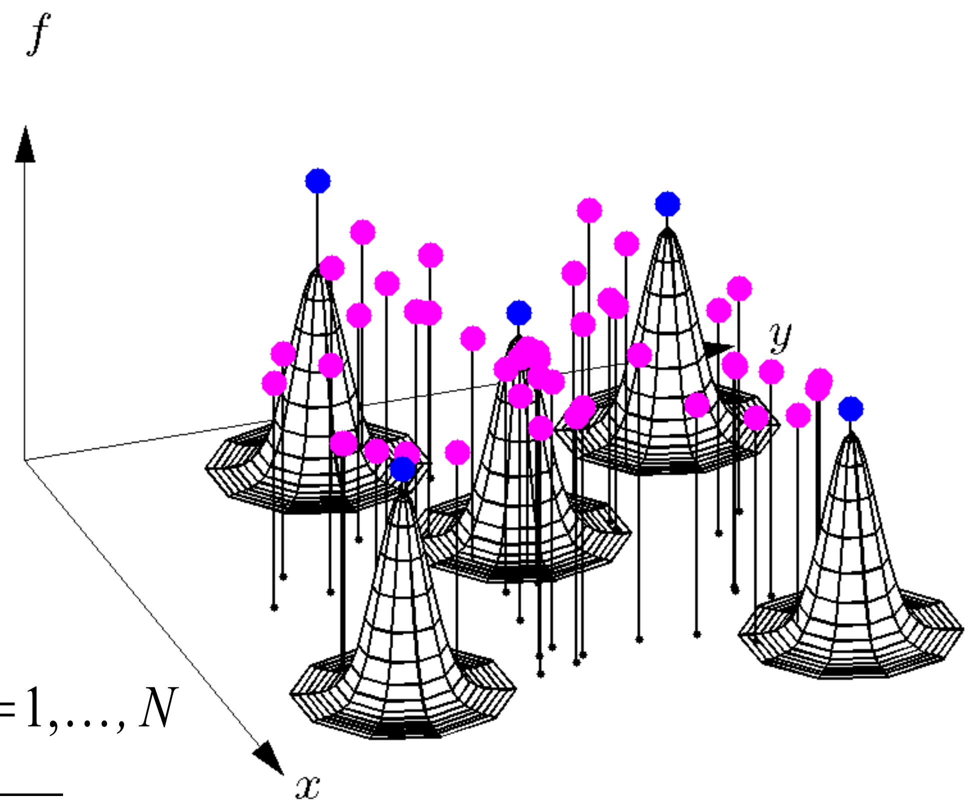

Interpolant:

$$s(\boldsymbol{x}) = \sum_{j=1}^{N} \beta_j \phi(\epsilon \|\boldsymbol{x} - \boldsymbol{x}_j\|), \quad s(\boldsymbol{x}_k) = f_k, \; k = 1, \ldots, N$$

where $\|\boldsymbol{x} - \boldsymbol{x}_j\| = \sqrt{(x - x_j)^2 + (y - y_j)^2}$

Introduction to RBFs via interpolation

Key idea: linear combination of translates and rotations of a single radial function:

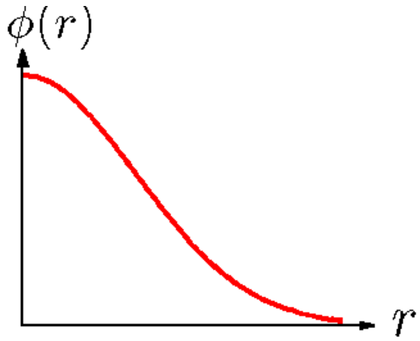

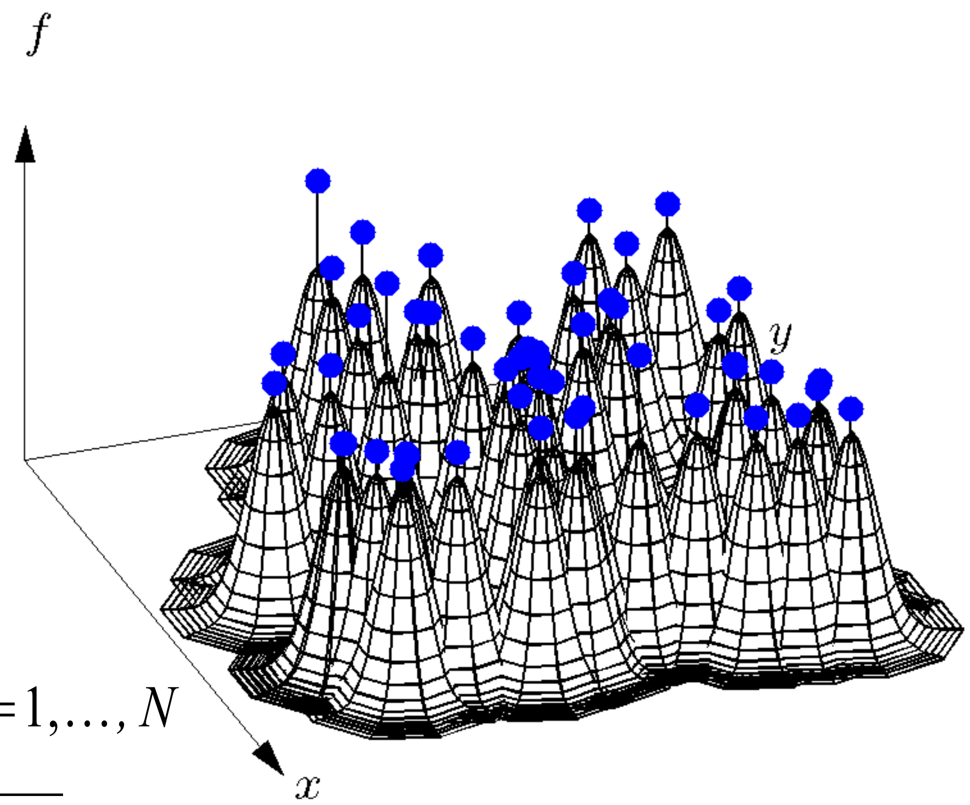

Interpolant:

$$s(\boldsymbol{x}) = \sum_{j=1}^{N} \beta_j \phi(\epsilon \|\boldsymbol{x} - \boldsymbol{x}_j\|), \quad s(\boldsymbol{x}_k) = f_k, \; k = 1, \ldots, N$$

where $\|\boldsymbol{x} - \boldsymbol{x}_j\| = \sqrt{(x - x_j)^2 + (y - y_j)^2}$

Introduction to RBFs via interpolation

Key idea: linear combination of translates and rotations of a single radial function:

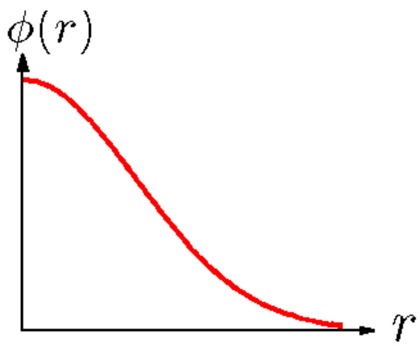

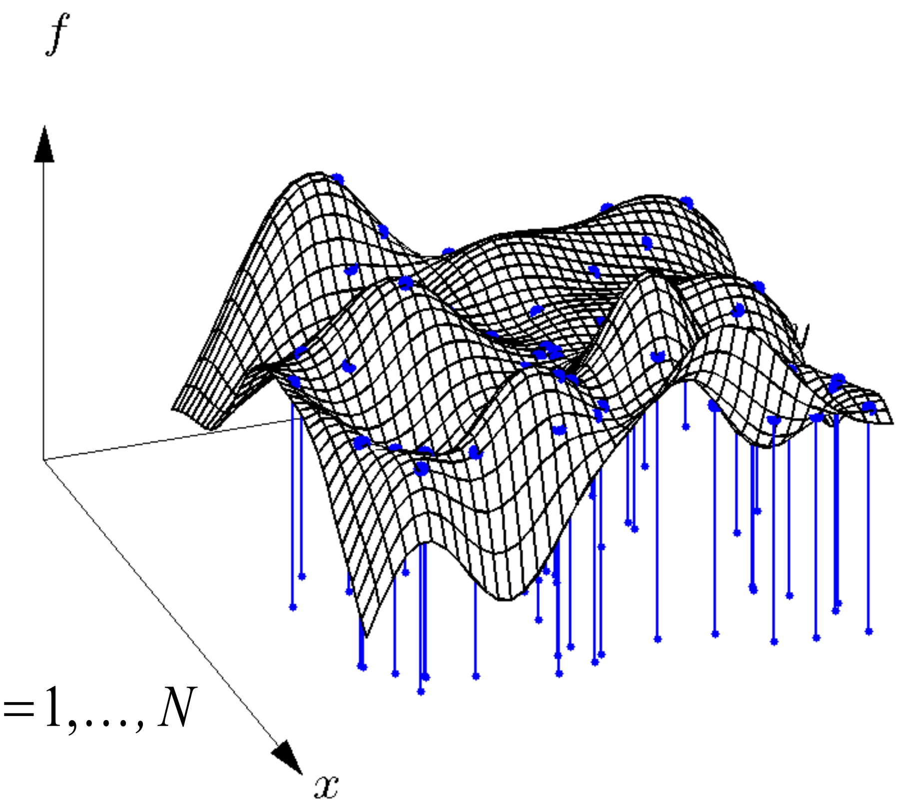

Interpolant:

$$s(\boldsymbol{x}) = \sum_{j=1}^{N} \beta_j \phi(\epsilon\|\boldsymbol{x}-\boldsymbol{x}_j\|), \quad s(\boldsymbol{x}_k) = f_k, \; k=1,\ldots,N$$

Linear system for expansion coefficients:

$$\begin{bmatrix} \phi(\epsilon\|\boldsymbol{x}_1-\boldsymbol{x}_1\|) & \phi(\epsilon\|\boldsymbol{x}_1-\boldsymbol{x}_2\|) & \cdots & \phi(\epsilon\|\boldsymbol{x}_1-\boldsymbol{x}_N\|) \\ \phi(\epsilon\|\boldsymbol{x}_2-\boldsymbol{x}_1\|) & \phi(\epsilon\|\boldsymbol{x}_2-\boldsymbol{x}_2\|) & \cdots & \phi(\epsilon\|\boldsymbol{x}_2-\boldsymbol{x}_N\|) \\ \vdots & \vdots & \ddots & \vdots \\ \phi(\epsilon\|\boldsymbol{x}_N-\boldsymbol{x}_1\|) & \phi(\epsilon\|\boldsymbol{x}_N-\boldsymbol{x}_2\|) & \cdots & \phi(\epsilon\|\boldsymbol{x}_N-\boldsymbol{x}_N\|) \end{bmatrix} \begin{bmatrix} \beta_1 \\ \beta_2 \\ \vdots \\ \beta_N \end{bmatrix} = \begin{bmatrix} f_1 \\ f_2 \\ \vdots \\ f_N \end{bmatrix},$$

Guaranteed positive-definite for appropriate $\phi(r)$

- Extends easily to higher dimensions, e.g. in 3-D: $\|\boldsymbol{x}-\boldsymbol{x}_j\| = \sqrt{(x-x_j)^2+(y-y_j)^2+(z-z_j)^2}$

Introduction to RBFs via interpolation

RBF Interpolant/approximant: $s(\boldsymbol{x}) = \sum_{j=1}^{N} \beta_j \phi(\epsilon \|\boldsymbol{x} - \boldsymbol{x}_j\|)$

- Classes and examples of radial functions:

<u>Piecewise smooth $\phi(r)$:</u>

r^3

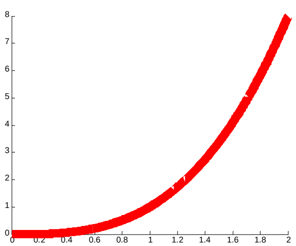

cubic

$r^2 \log r$

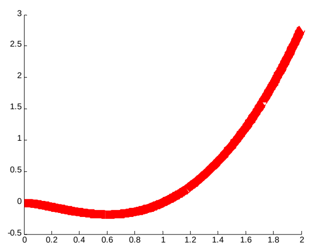

TP spline

$(1-r)_+^3(3r+1)$

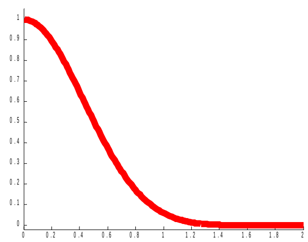

Wendland

<u>Infinitely smooth $\phi(r)$::</u>

e^{-r^2}

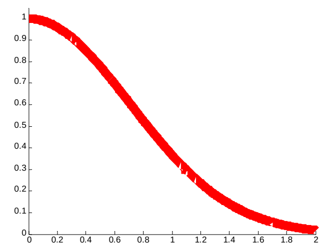

Gaussian

$\dfrac{1}{1+r^2}$

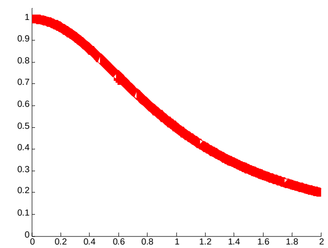

Inverse quadratic

$\sqrt{1+r^2}$

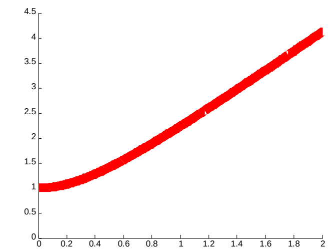

multiquadric

<u>Bottom line regarding RBFs:</u>

1. High algorithmic simplicity
2. Independent of dimension
3. Independent of coordinate system

Shallow water wave equations on a rotating sphere

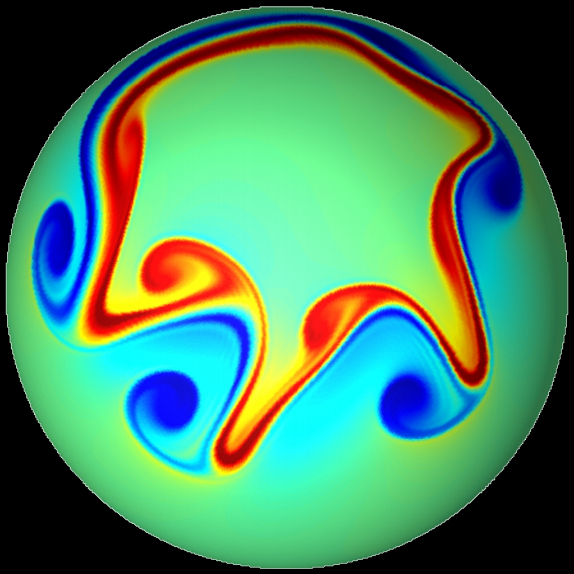

Collaborators:

Natasha Flyer, Institute for Mathematics Applied to Geosciences, NCAR
Erik Lehto, Dept. of Information Technology, Uppsala University, Sweden
Sébastien Blaise, Institute for Mathematics Applied to Geosciences, NCAR
Amik St-Cyr, Royal Dutch Shell, Houston, Texas

RBFs for spherical geometries

Interpolation in a box

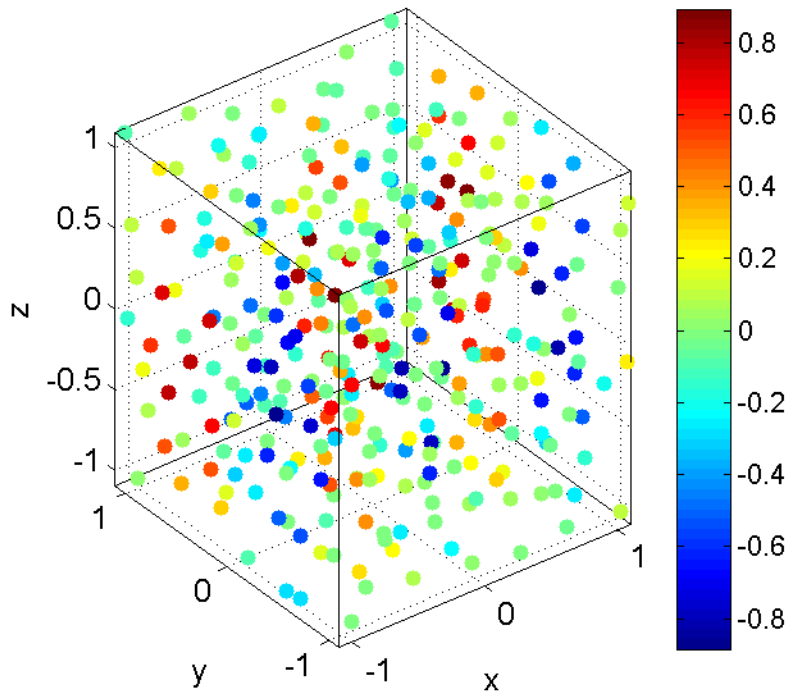

Interpolation on the sphere

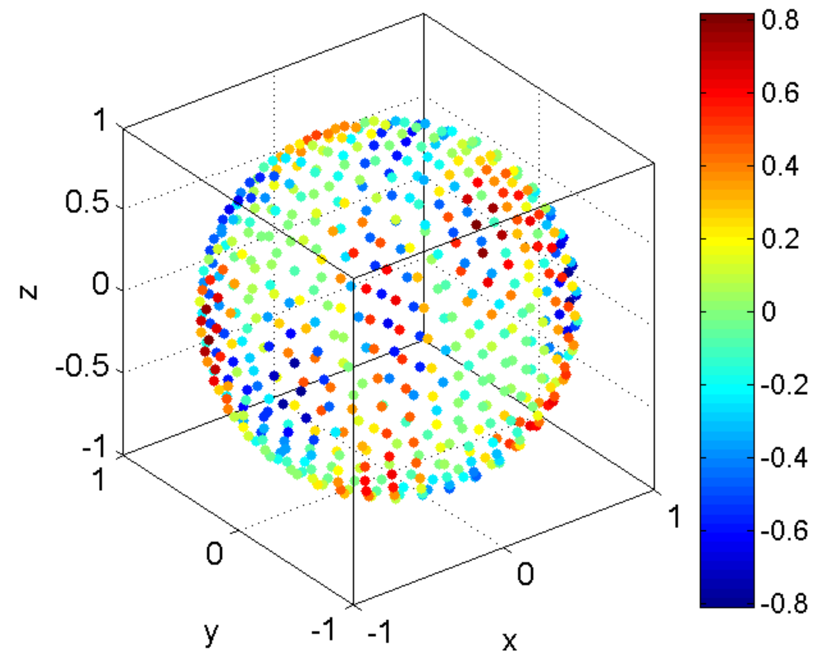

Interpolant does not change:

$$s(\boldsymbol{x}) = \sum_{j=1}^{N} \beta_j \phi(\epsilon \| \boldsymbol{x} - \boldsymbol{x_j} \|), \quad s(\boldsymbol{x_k}) = f_k, \; k = 1, \ldots, N$$

Examples of different optimal point sets on the sphere

Icosahedral

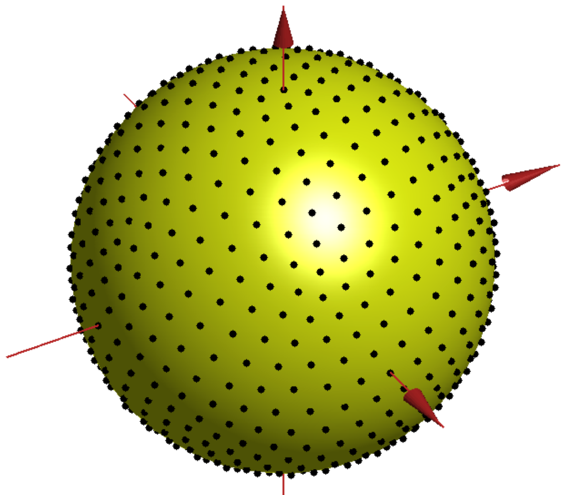

J. Baumgardner and P. Frederickson, Icosehedral discretization of the two- sphere, *SIAM J. Sci. Comput.* 22 (1985), 1107–1115.

Equal Area

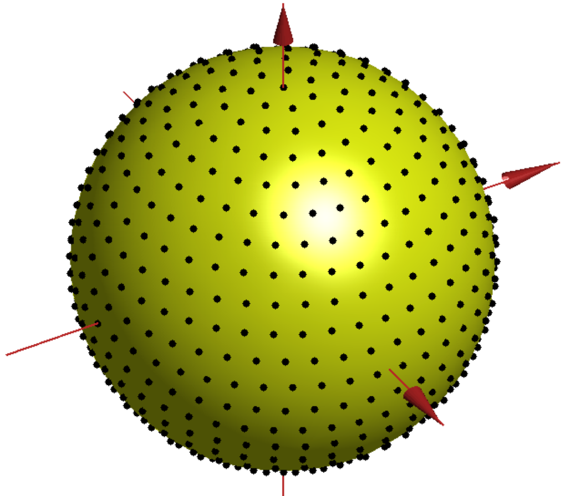

E.B. Saff and A.B.J. Kuijlaars. Distributing many points on a sphere. *Mathematical Intelligencer*, 19(1), 5-11, 1997.

Fibonacci

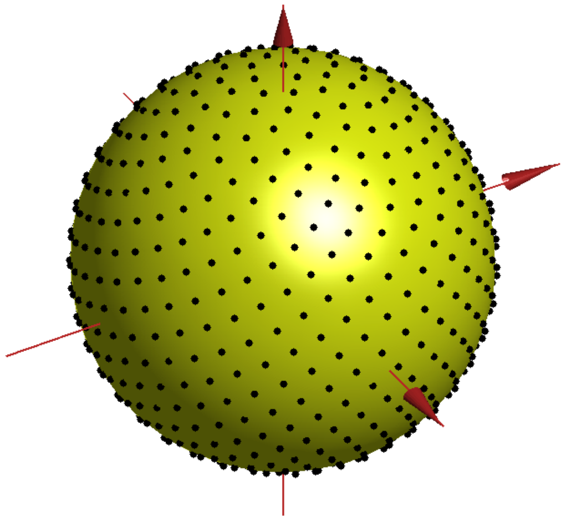

R. Swinbank and R.J. Purser. Fibonacci girds: A novel approach to global modeling. *Quart. J. Roy. Meteor. Soc.,* 132, 1769-1793, 2006.

Minimum Energy

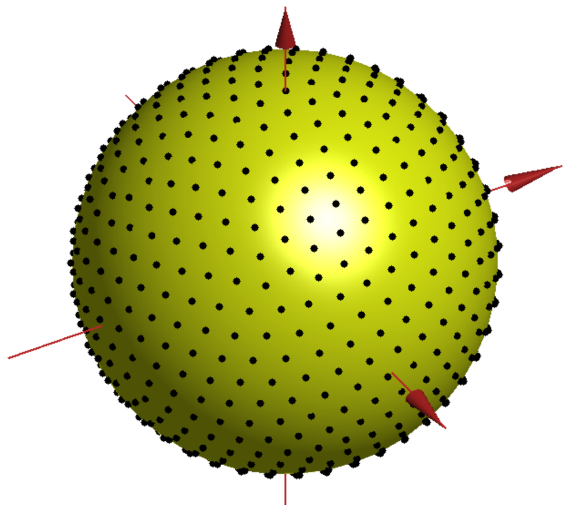

- D. P. Hardin and E. B. Saff. Discretizing manifolds via minimum energy points. *Notices Amer. Math. Soc.*, 51:1186–1194, 2004.
- R.S. Womersley and I.H. Sloan, `http://web.maths.unsw.edu.au/~rsw/Sphere/`

Shallow water equations (SWE) on a rotating sphere

- Model for the nonlinear dynamics of a shallow, hydrostatic, homogeneous, and inviscid fluid layer.

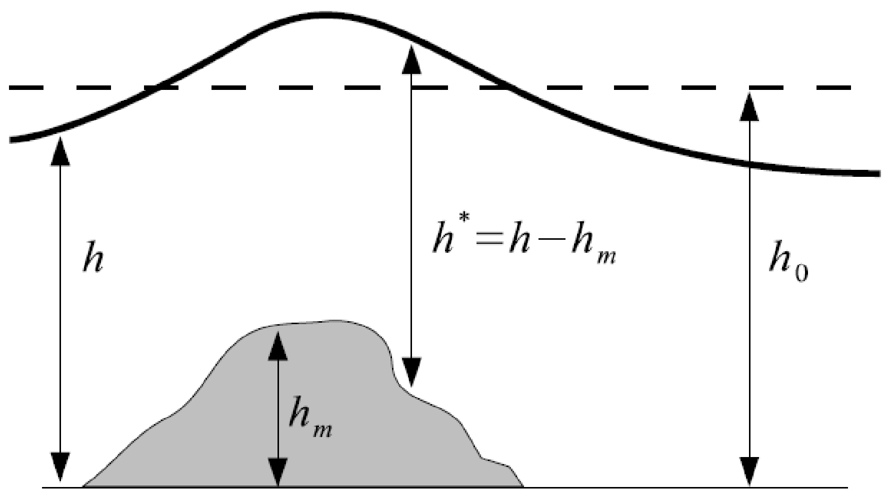

- Idealized test-bed for the horizontal dynamics of all 3-D global climate models.

Equations	Momentum	Transport
Spherical coordinates	$\dfrac{\partial \mathbf{u}_s}{\partial t} + \mathbf{u}_s \cdot \nabla_s \mathbf{u}_s + f\hat{\mathbf{k}} \times \mathbf{u}_s + g\nabla_s h = 0$	$\dfrac{\partial h^*}{\partial t} + \nabla_s \cdot (h^* \mathbf{u}_s) = 0$
Cartesian coordinates	$\dfrac{\partial \mathbf{u}_c}{\partial t} + P \begin{bmatrix} (\mathbf{u}_c \cdot P\nabla_c)u_c + f(\mathbf{x} \times \mathbf{u}_c) \cdot \hat{\mathbf{i}} + g(P\hat{\mathbf{i}} \cdot \nabla_c)h \\ (\mathbf{u}_c \cdot P\nabla_c)v_c + f(\mathbf{x} \times \mathbf{u}_c) \cdot \hat{\mathbf{j}} + g(P\hat{\mathbf{j}} \cdot \nabla_c)h \\ (\mathbf{u}_c \cdot P\nabla_c)w_c + f(\mathbf{x} \times \mathbf{u}_c) \cdot \hat{\mathbf{k}} + g(P\hat{\mathbf{k}} \cdot \nabla_c)h \end{bmatrix} = 0$	$\dfrac{\partial h^*}{\partial t} + (P\nabla_c) \cdot (h^* \mathbf{u}_c) = 0$

Singularity at poles!

Smooth over entire sphere!

RBF discretization for SWE on a rotating sphere

Governing equations:

$$\frac{\partial \mathbf{u}_c}{\partial t} = -P \begin{bmatrix} (\mathbf{u}_c \cdot P\nabla_c)u_c + f(\mathbf{x} \times \mathbf{u}_c) \cdot \hat{\mathbf{i}} + g(P\hat{\mathbf{i}} \cdot \nabla_c)h \\ (\mathbf{u}_c \cdot P\nabla_c)v_c + f(\mathbf{x} \times \mathbf{u}_c) \cdot \hat{\mathbf{j}} + g(P\hat{\mathbf{j}} \cdot \nabla_c)h \\ (\mathbf{u}_c \cdot P\nabla_c)w_c + f(\mathbf{x} \times \mathbf{u}_c) \cdot \hat{\mathbf{k}} + g(P\hat{\mathbf{k}} \cdot \nabla_c)h \end{bmatrix} \qquad \frac{\partial h^*}{\partial t} = -(P\nabla_c) \cdot (h^* \mathbf{u}_c)$$

Collocation nodes

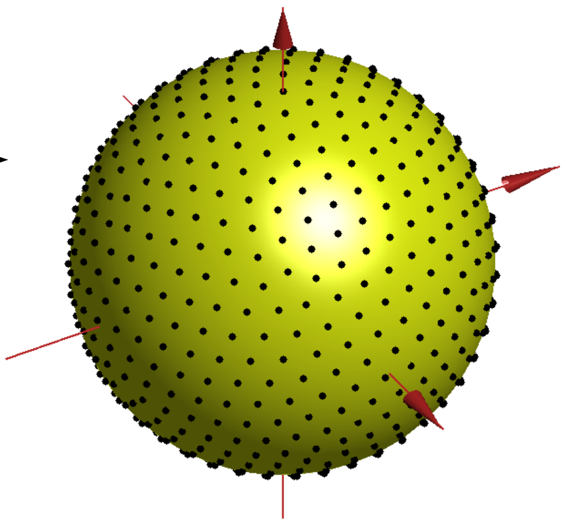

Procedure: Collocation and Method-of-Lines:

1. Choose some "nice" discretization of the sphere:

2. Approximate continuous differential operators at the nodes with discrete operators (differentiation matrices) using RBF interpolants

$$s(\boldsymbol{x}) = \sum_{j=1}^{N} \beta_j \phi(\epsilon \|\boldsymbol{x} - \boldsymbol{x}_j\|)$$

3. Replace unknowns with pointwise values and continuous operators with differentiation matrices.

   - Governing equations are satisfied pointwise at the nodes (collocation).

4. Advance the system in time using some "standard" ODE method.

Numerical Example I

Forcing terms added to the shallow water equations to generate a flow that mimics a short wave trough embedded in a westerly jet. (Test case 4 of Williamson *et. al.* 1992)

[Initial velocity field]

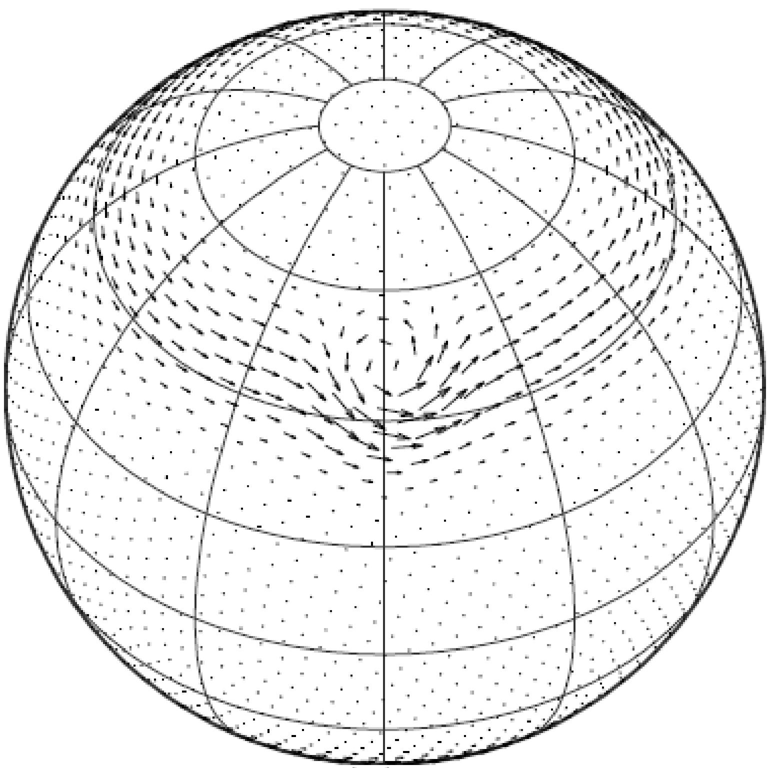

(a)

[Initial geopotential height field]

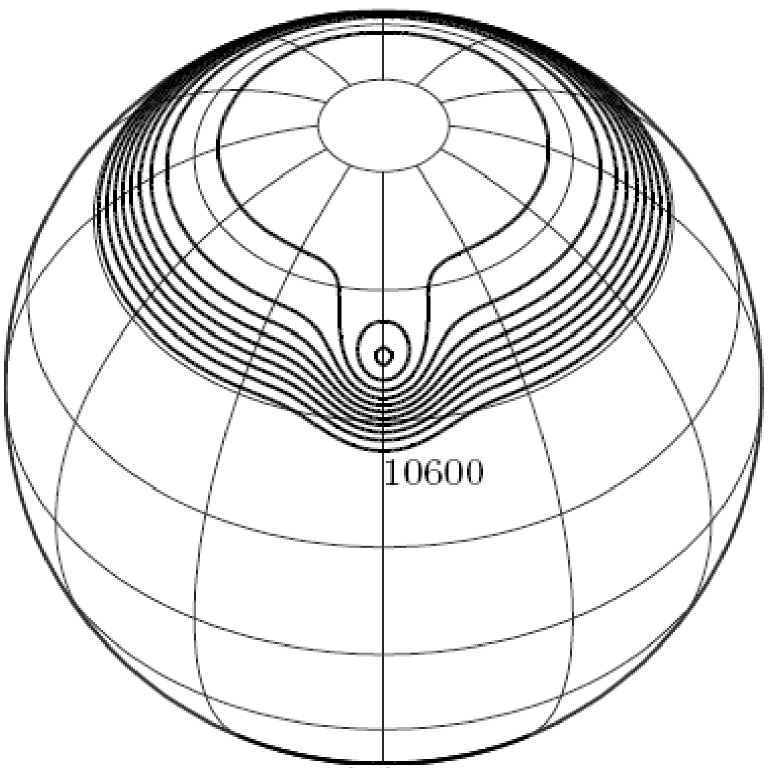

(b)

Errors after trough travels once around the sphere

- Results of the RBF Shallow Water Model:
  (N. Flyer and G.B. Wright. *Proc. R. Soc. A*, 2009)

Error as a function of time and N

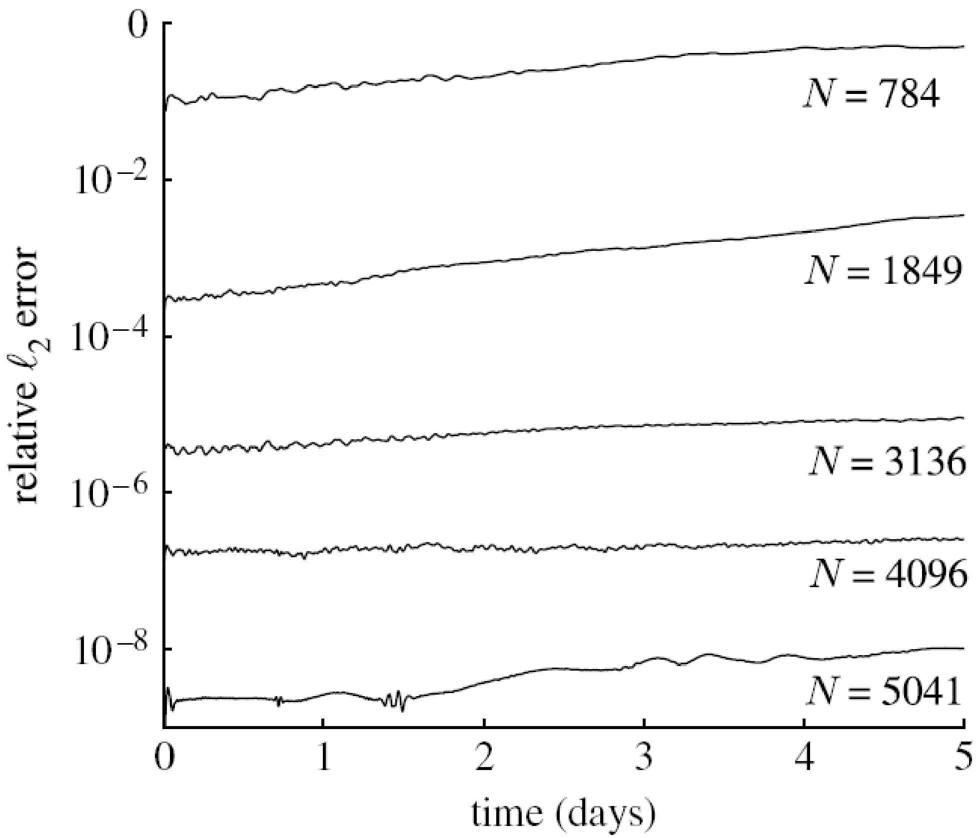

Error height field, $t = 5$ days

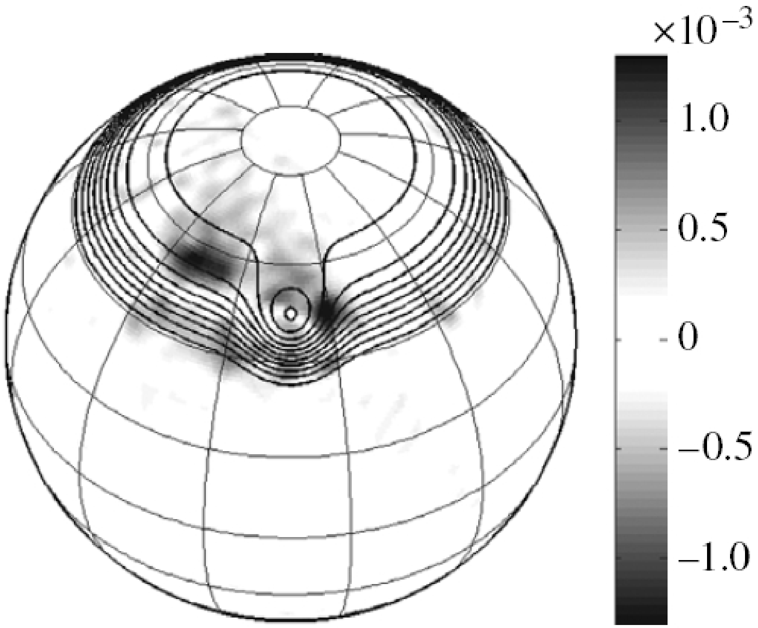

$N = 3136$, white $< 10^{-5}$
Error (exact - numerical)

Comparison with commonly used methods

Method	N	Time step	Relative ℓ_2 error
RBF	4,096	8 minutes	2.5×10^{-6}
	5,041	6 minutes	1.0×10^{-8}
Sph. Harmonic	8,192	3 minutes	2.0×10^{-3}
Double Fourier	32,768	90 seconds	4.0×10^{-4}
Spect. Element	24,576	45 seconds	4.0×10^{-5}

Time-step for RBF method: Temporal Errors = Spatial Errors
Time-step for other methods: Limited by numerical stability

- RBF method runtime in MATLAB using 2.66 GHz Xeon Processor

N	Runtime per time step (sec)	Total Runtime
4,096	0.41	6 minutes
5,041	0.60	12 minutes

For much higher numerical accuracy, RBFs uses less nodes & larger time steps

New discretization strategy: RBF-FD Method

- Key Idea: Construct an approximation to the differential operators at a node locally using an RBF interpolant defined only on *m* surrounding nodes.

Illustration:

4 stencils to approximate derivatives

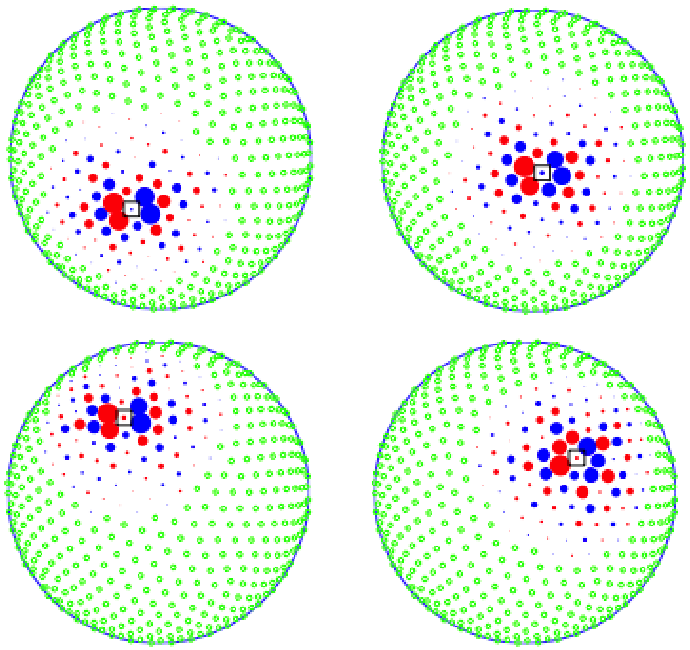

Differentiation matrix for *N*=25000 nodes

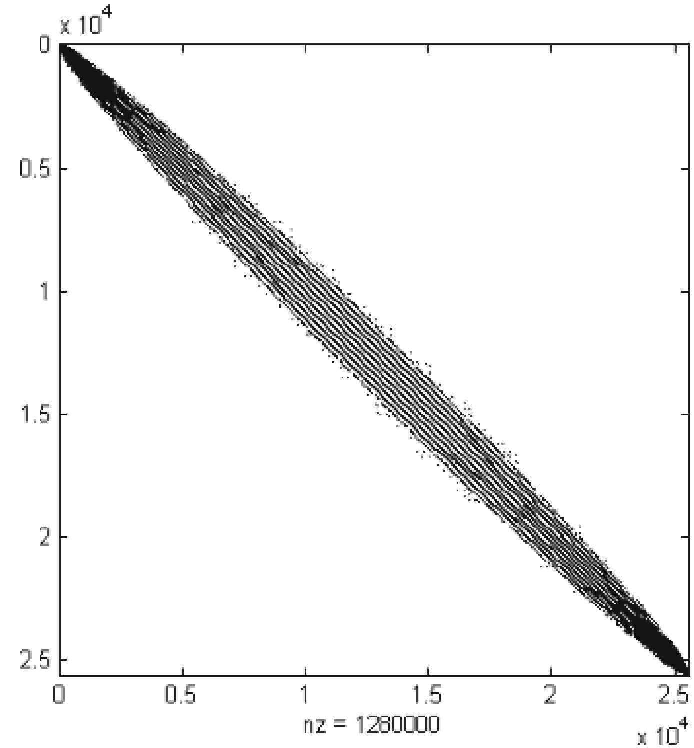

0.2% full

- Similarities to how finite differences (FD) are constructed.
- Key difference is that this works for *scattered nodes.*
- Call this method the RBF-FD method.
- *Results in a fast, scalable method.*

Numerical Example II: RBF-FD method

(Flyer, Lehto, Blaise, Wright, and St-Cyr. Submitted, 2011)

Flow over a conical mountain (Test case 5 of Williamson *et. al.* 1992)

Height field at t=0 days

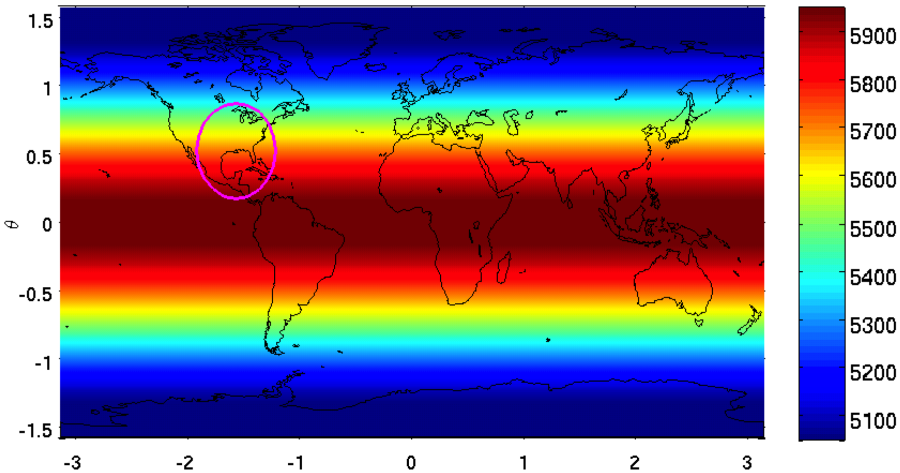

Height field at t=15 days

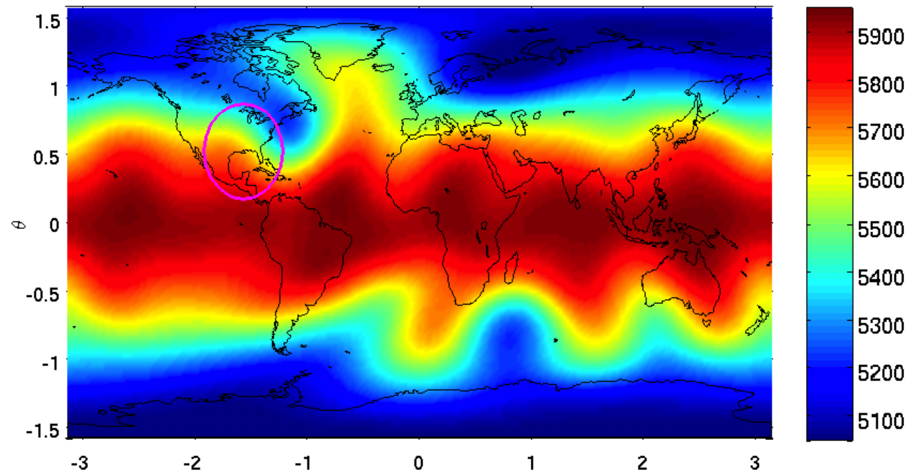

Simulation

Convergence comparison: 3 reference solutions

Convergence plot RBF-FD with stencil size of m=31

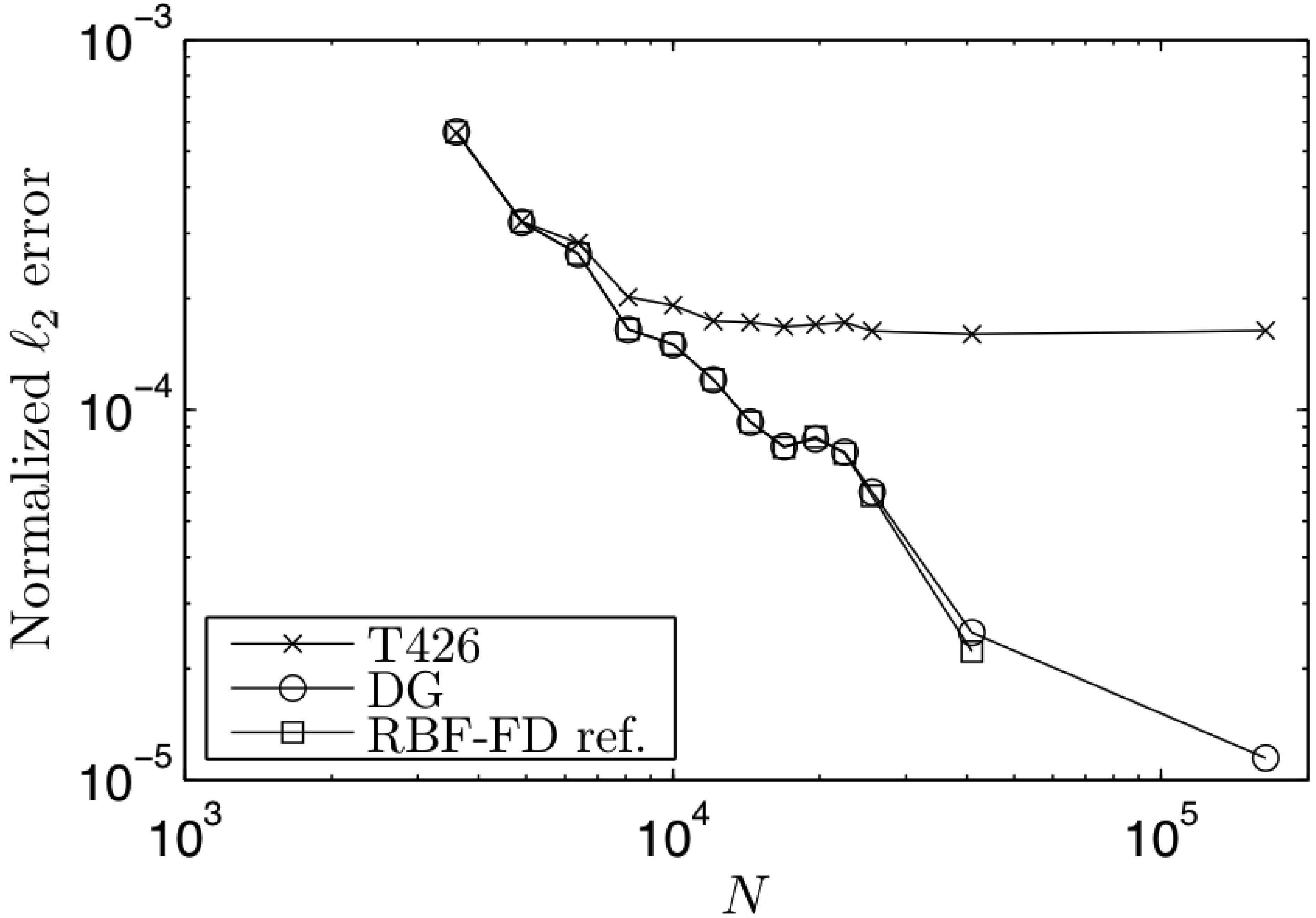

× Standard Literature/Comparison: NCAR's Sph. Har. T426, Resolution ≈ 30 km at equator

○ New Model at NCAR Discontinuous Galerkin – Spectral Element, Resolution ≈ 30 km

□ RBF-FD model, Resolution ≈ 60 km

Error vs. runtime comparison

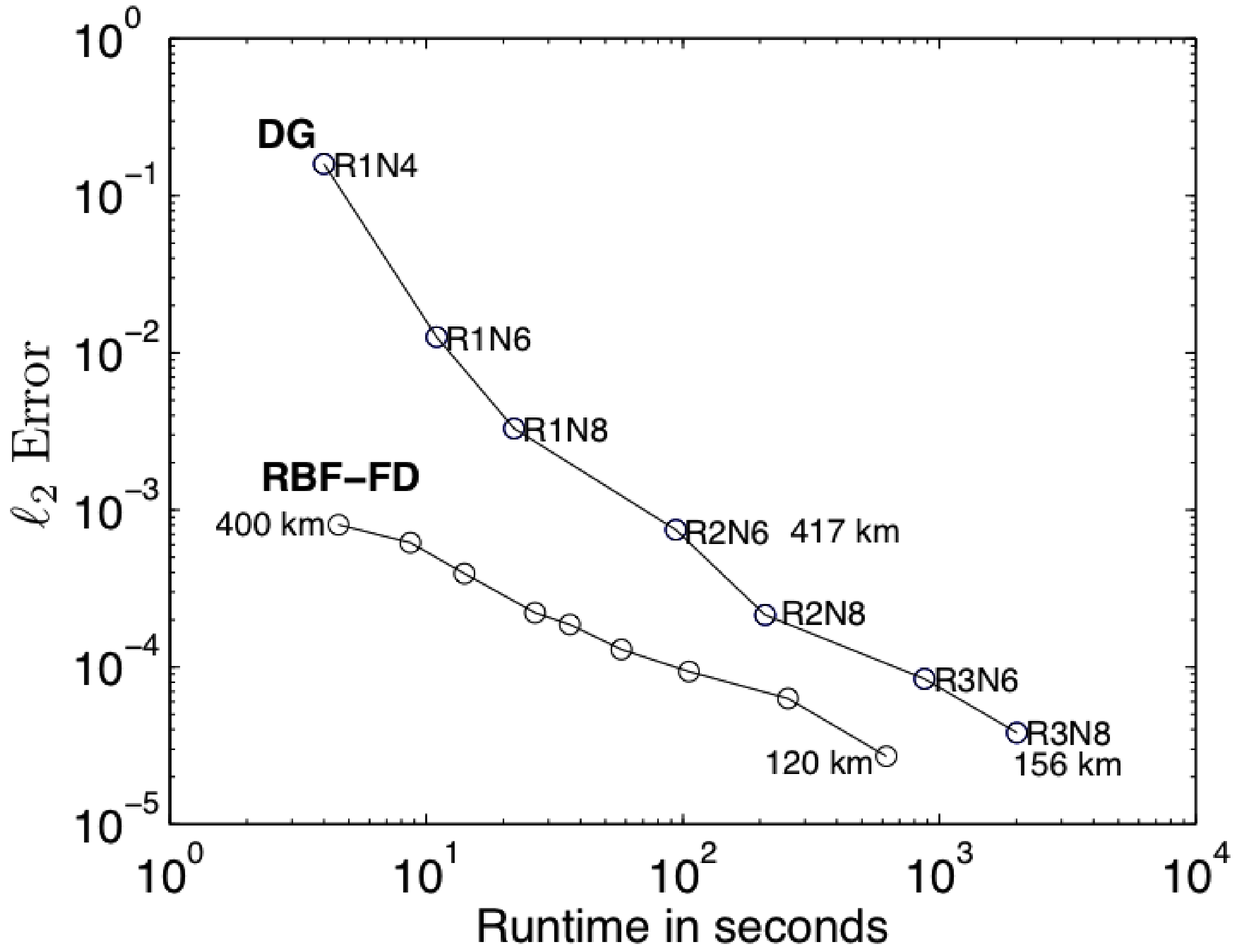

Machine: MacBook Pro, Intel i7 2.2 GHz, 8 GB Memory

Numerical Example III: RBF-FD method

- Evolution of a highly non-linear wave: (Test case from Galewsky et. al. *Tellus*, 2004)
- RBF-FD method with N=163,842 nodes and m=31 point stencil.

Visualization of the relative vorticity

Day 3

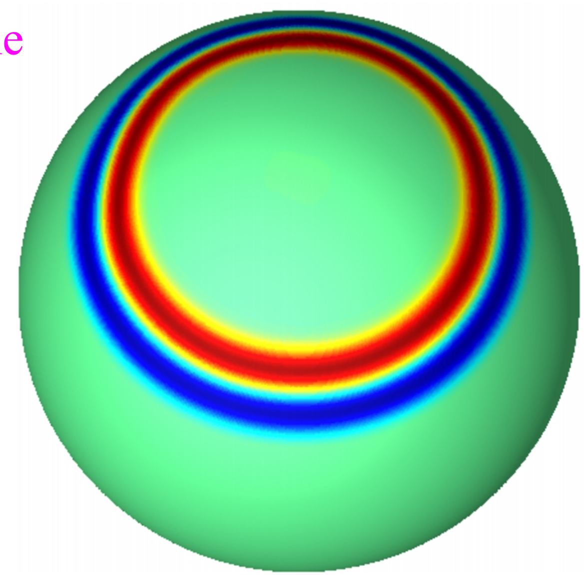

Day 4

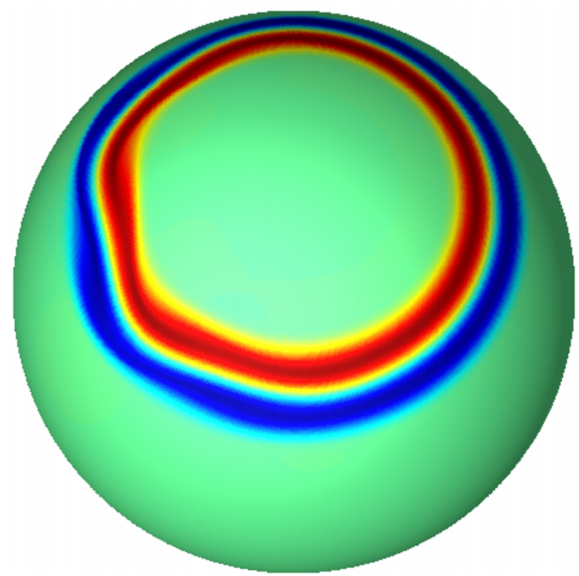

Day 5

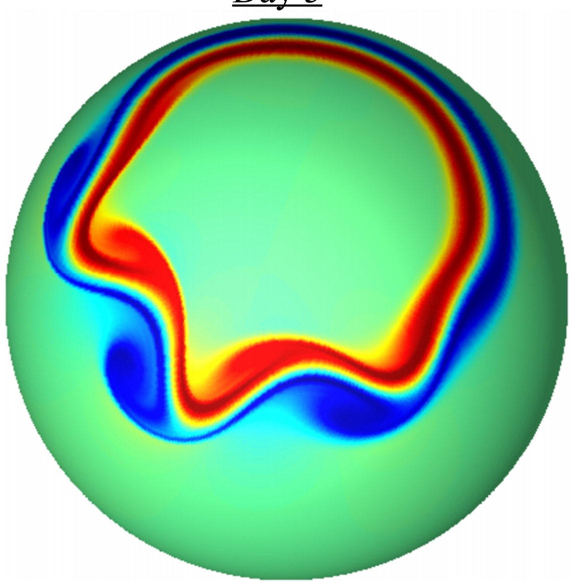

Day 6

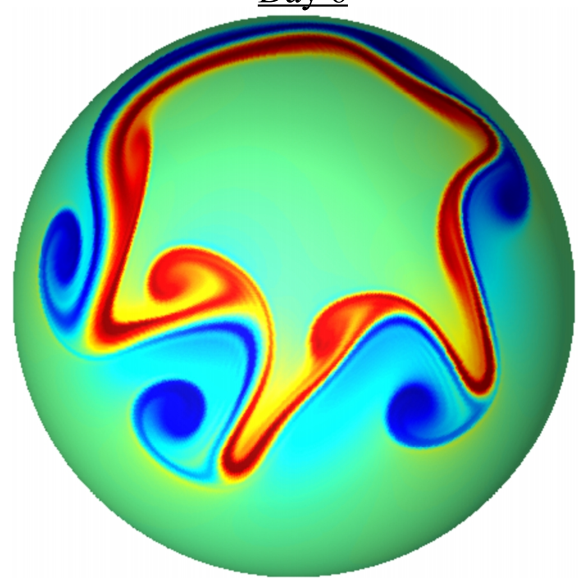

Thermal convection in a 3D spherical shell with applications to the Earth's mantle.

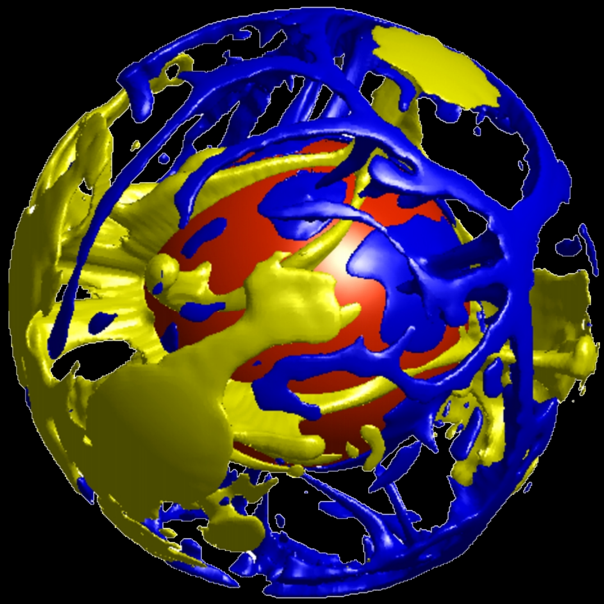

Collaborators

Natasha Flyer, Institute for Mathematics Applied to Geosciences, NCAR
David A. Yuen, Department of Geology and Geophysics, University of Minnesota
Louise H. Kellogg, Dept. of Geology, UC Davis
Pierre-Andre Arrial, Dept. of Geology, UC Davis
Gordon Erlebacher, School of Computational Science and IT, Florida State University

Simulating convection in the Earth's mantle

(Wright, Flyer, and Yuen. *Geochem. Geophys. Geosyst.*, 2010)

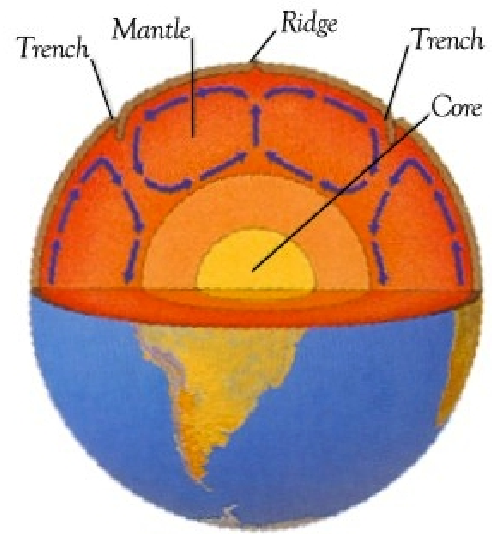

- Model assumptions:
  1. Fluid is incompressible
  2. Viscosity of the fluid is constant
  3. Boussinesq approximation
  4. Infinite Prandtl number, $\mathrm{Pr} = \dfrac{\text{kinematic viscosity}}{\text{thermal diffusivity}} \rightarrow \infty$

- Non-dimensional Equations:

$$\begin{aligned} \nabla \cdot \mathbf{u} &= 0 \quad \text{(continuity)}, \\ \nabla^2 \mathbf{u} + \mathrm{Ra}\, T\, \hat{\mathbf{r}} - \nabla p &= 0 \quad \text{(momentum)}, \\ \frac{\partial T}{\partial t} + \mathbf{u} \cdot \nabla T - \nabla^2 T &= 0 \quad \text{(energy)}. \end{aligned}$$

- Boundary conditions:

  Velocity: impermeable and shear-stress free
  Temperature (isothermal): $T = 1$ at core mantle bndry., $T = 0$ at crust mantle bndry.

- Rayleigh, Ra, number governs the dynamics.
- Model for Rayleigh-Bénard convection

Discretization of the equations

- Use a hybrid RBF-Pseudospectral method
- Collocation procedure using a 2+1 approach with
  - N RBF nodes on each spherical surface (θ and λ directions) and
  - M Chebyshev nodes in the radial direction.

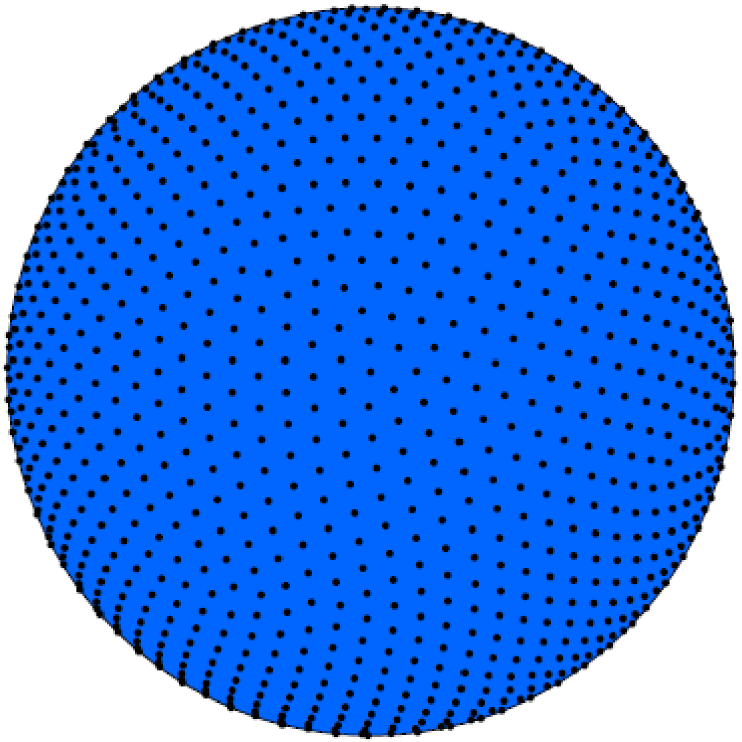

N RBF nodes (ME) on a spherical surface

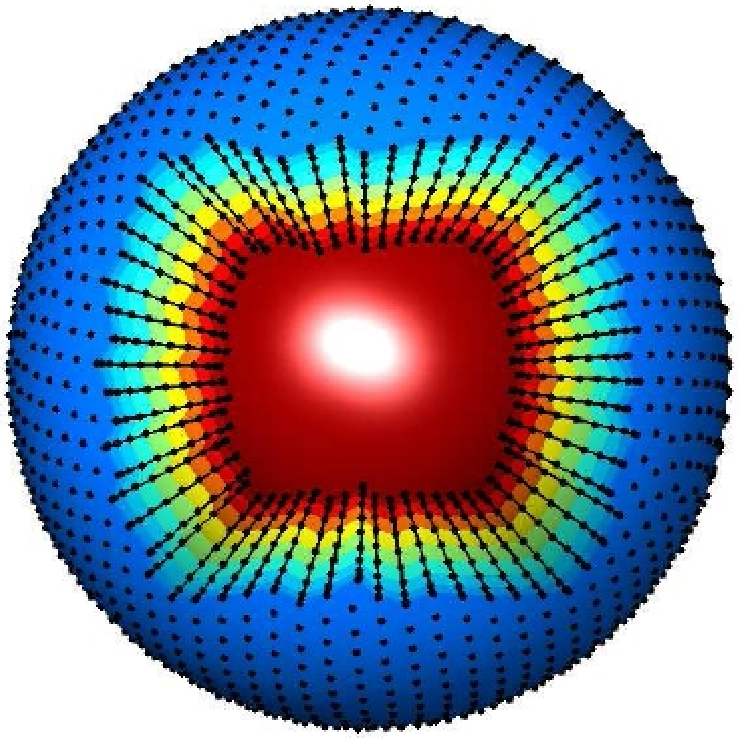

3-D node layout showing *M* Chebyshev nodes in radial direction

Ra=7000 benchmark: validation of method

Perturbation initial condition: $0.01\left[Y_4^0(\theta,\lambda)+\frac{5}{7}Y_4^4(\theta,\lambda)\right]$

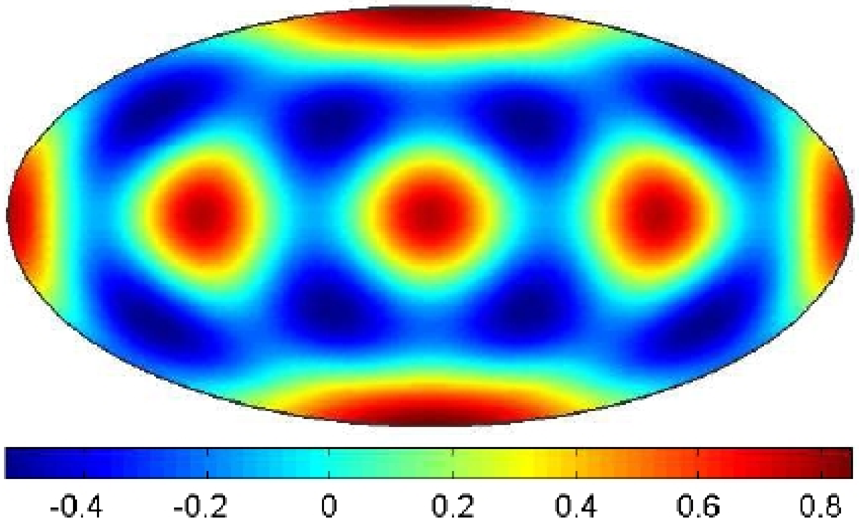

Steady solution:

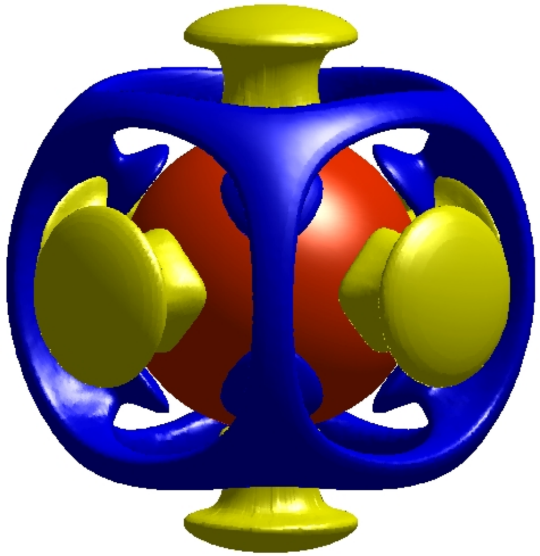

N = 1600 nodes on each spherical shell
M = 23 shells
Blue=downwelling, Yellow= upwelling, Red=core

- Comparisons against main previous results from the literature:

Method	No of nodes	Nu_{outer}	Nu_{innner}	$<V_{RMS}>$	$<T>$
Finite volume	663,552	3.5983	3.5984	31.0226	0.21594
Finite elements (CitCom)	393,216	3.6254	3.6016	31.09	0.2176
Finite differences (Japan)	12,582,912	3.6083		31.0741	0.21639
Spherical harmonics -FD	552,960	3.6086		31.0765	0.21582
Spherical harmonics -FD	Extrapolated	3.6096		31.0821	0.21577
RBF-Chebyshev	36,800	3.6096	3.6096	31.0820	0.21578

Nu = ratio of convective to conductive heat transfer across a boundary

High Ra Number: Comparing two novel simulations

Novelty: First mantle convection model run on a Graphics Processing Unit (GPU)
Strength: Simulation run times up to 15 times faster
Drawback: Second-order, very dissipative, non-spherical geometry

Degrees of freedom: 32 million
Time step ≈ 34,000 years

$\boxed{Ra = 10^7}$

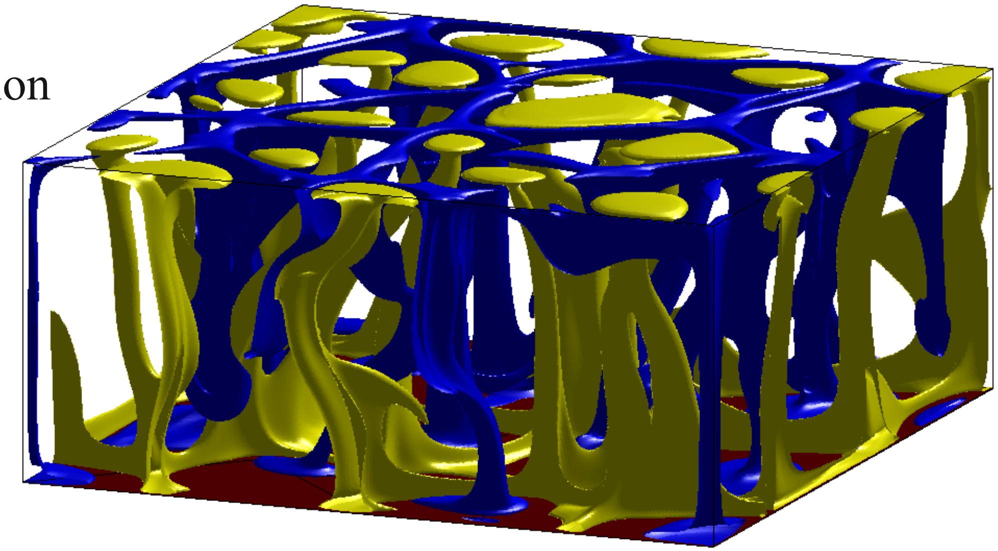

Blue=downwelling,
Yellow= upwelling,
Red=core

Novelty: Largest RBF simulation
Strength: Only fully spectrally accurate simulation
Drawback: Computationally slow

Degrees of freedom: 531,441
Time step ≈ 34,000 years

$\boxed{Ra = 10^6}$

Simulation

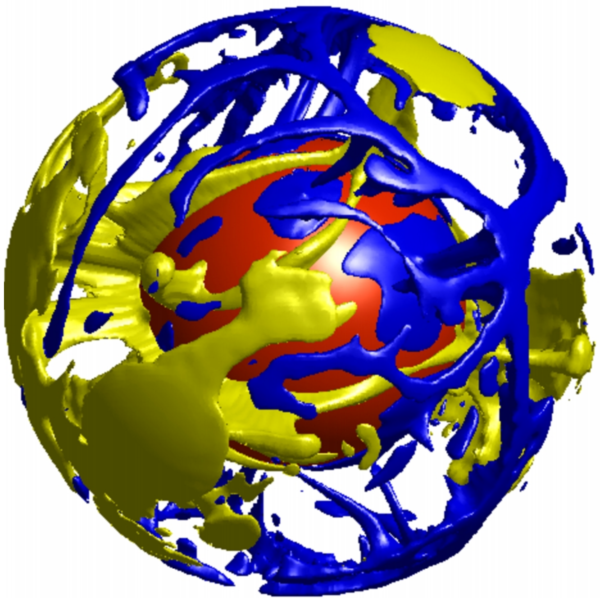

t=4.5 times the age of the earth

An investigation of low Ra number instabilities

Perturb standard cubic test $$T(r,\theta,\lambda) = \left[Y_4^0(\theta,\lambda) + (1-\delta)\frac{5}{7}Y_4^4(\theta,\lambda)\right]\sin\left(\pi\frac{r-R_\mathrm{i}}{R_\mathrm{o}-R_\mathrm{i}}\right)$$

Ra = 70K, Simulation time t=0.3 (≈18 times age of the Earth)

Steady flow

δ=0

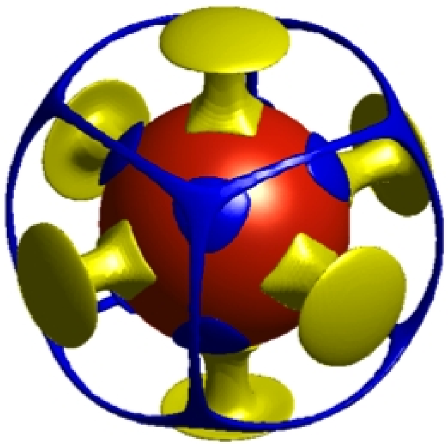

δ=0.06

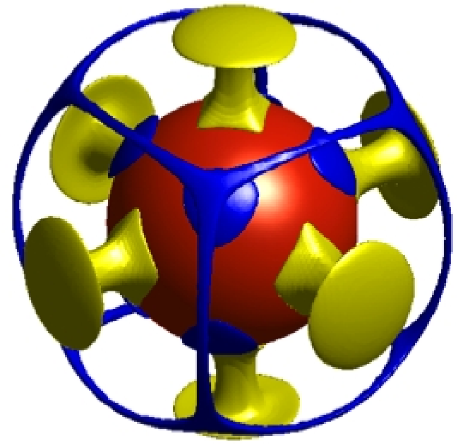

δ=0.07

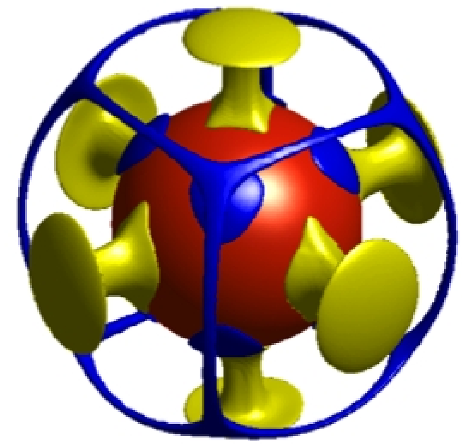

Unsteady flow

δ=0.075

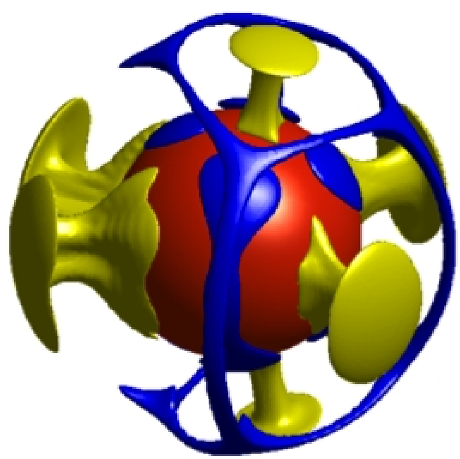

δ=0.10

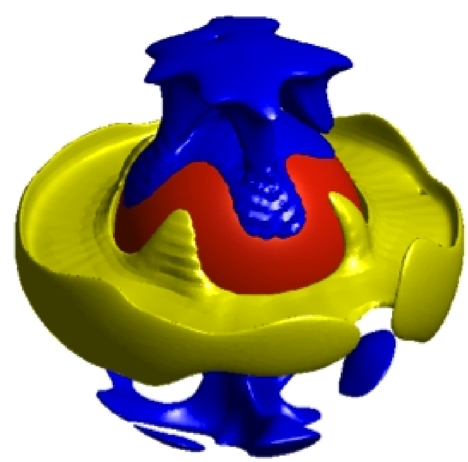

Joint work with Natasha Flyer, Louise Kellogg, Pierre-Andre Arrial, and Dave Yuen

Current focus

- Improving computational efficiency: use RBF generated finite differences (RBF-FD)

Illustration:

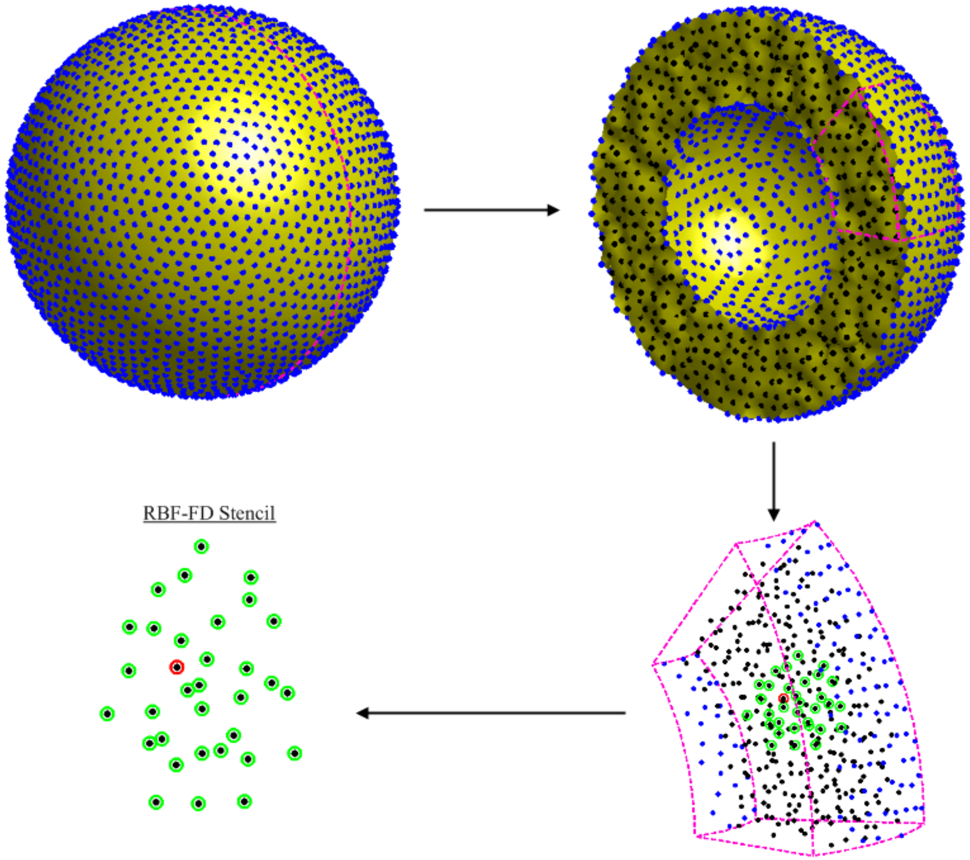

- Extend model to handle more realistic physics (e.g. variable viscosity, mantle layering).

Joint work Natasha Flyer, Gordon Erlebacher, Evan Bollig (graduate student), Greg Barnett (graduate student)

Reconstruction and decomposition vector fields.

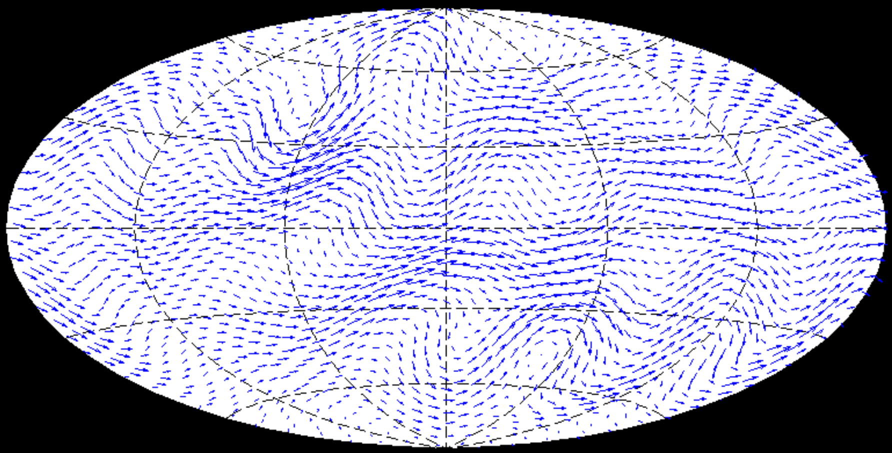

Collaborators

Edward J Fuselier, Dept. of Mathematics, High Point University
Francis J. Narcowich, Dept. of Mathematics, Texas A&M
Joseph D. Ward, Dept. of Mathematics, Texas A&M
Uwe Harlander, Dept. Aerodynamics and Fluid Mechanics, BTU Cottbus

Helmholtz-Hodge Theorem

- Theorem: Any vector field tangent to the sphere can be *uniquely* decomposed into surface divergence-free and surface curl-free components:

$$\begin{aligned} \mathbf{u}(\mathbf{x}) &= \mathbf{u}_{\text{div}}(\mathbf{x}) + \mathbf{u}_{\text{curl}}(\mathbf{x}) \\ &= Q_{\mathbf{x}}\nabla\psi(\mathbf{x}) + P_{\mathbf{x}}\nabla\chi(\mathbf{x}) \end{aligned}$$

$$\psi = \text{stream function and } \chi = \text{velocity potential}$$

- Example:

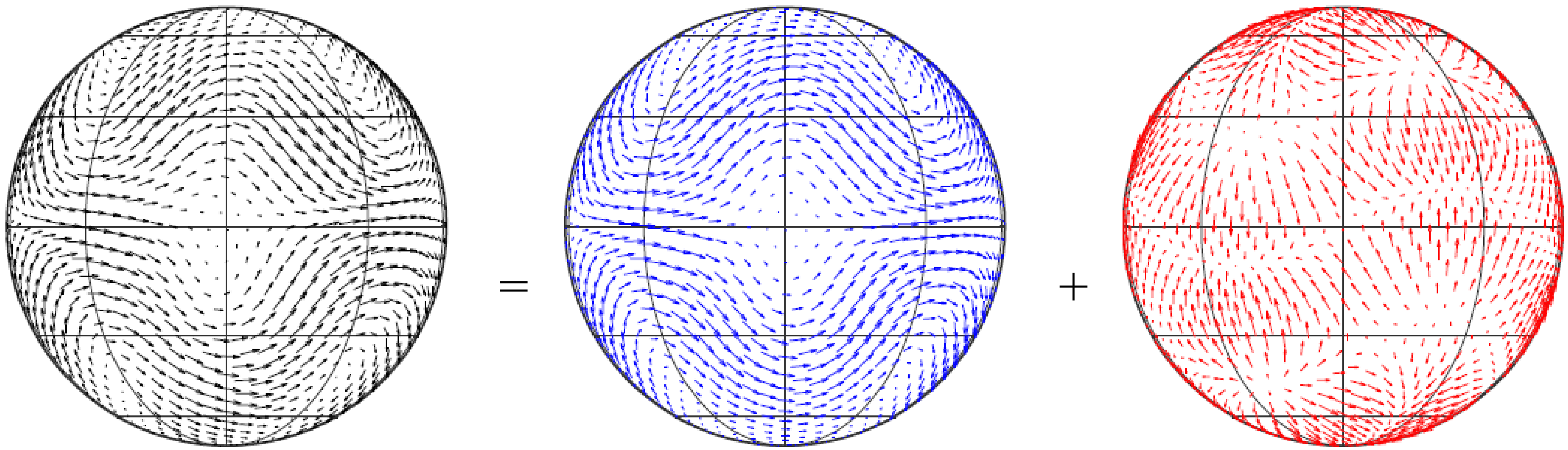

Goal: Construct an RBF-type interpolant that mimics the Helmholtz-Hodge decomposition.

Example: decomposition of a atmospheric velocity field

- Test case 5 (flow over an isolated mountain) from Williamson *et. al.* JCP (1992).

Height field t=15 days

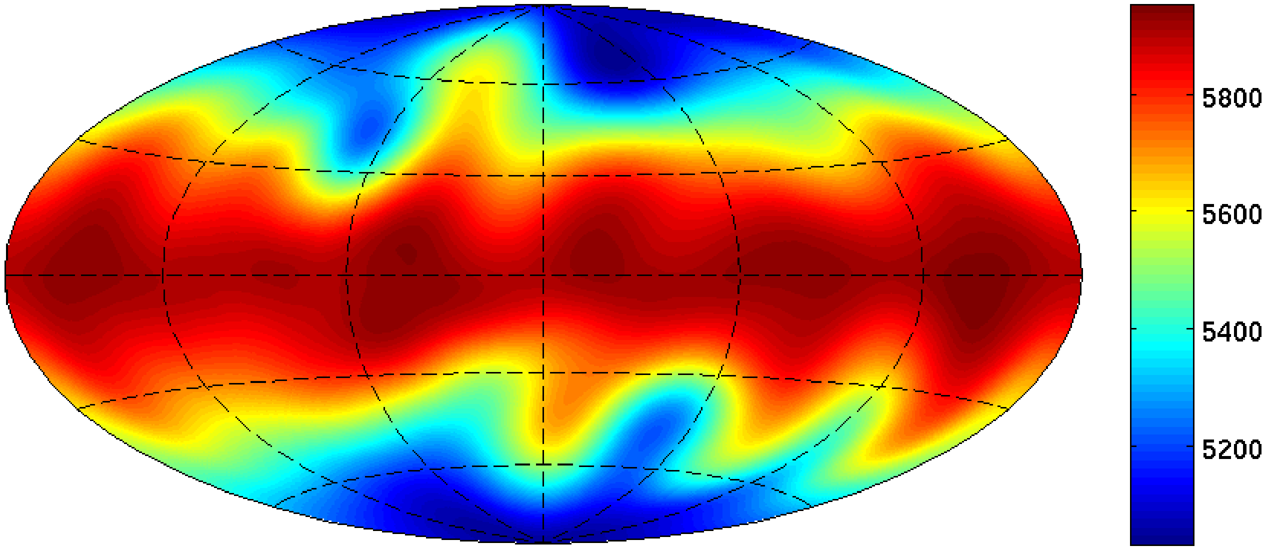

Velocity field **u** t=15 days

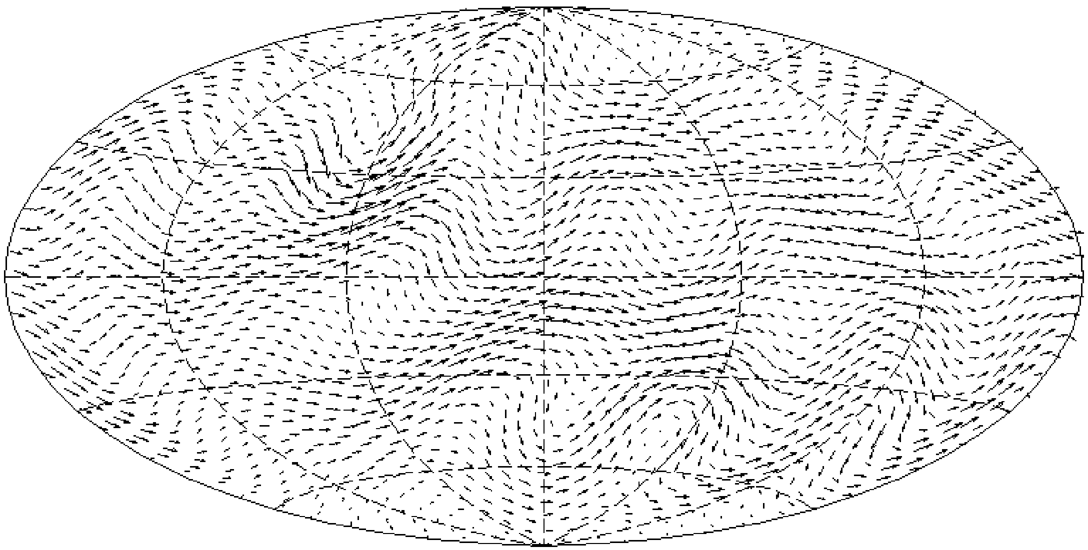

Example: decomposition of a geophysical velocity field

- Test case 5 (flow over an isolated mountain) from Williamson *et. al.* JCP (1992).

RBF reconstructed div-free velocity field t=15 days

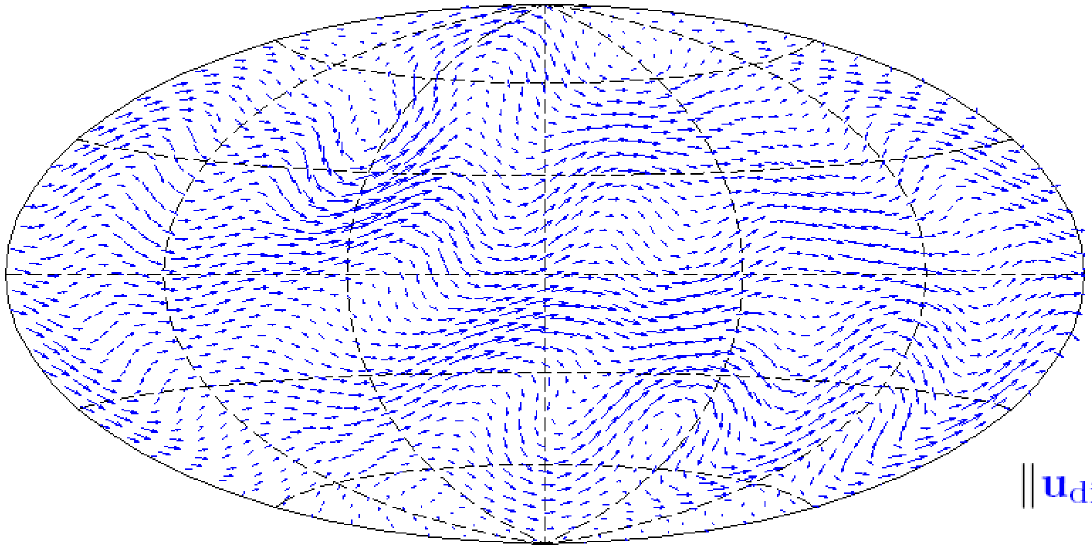

$\|\mathbf{u}_{\text{div}}\|_2 = 40.3 \text{ m/s}$

RBF reconstructed curl-free velocity field t=15 days

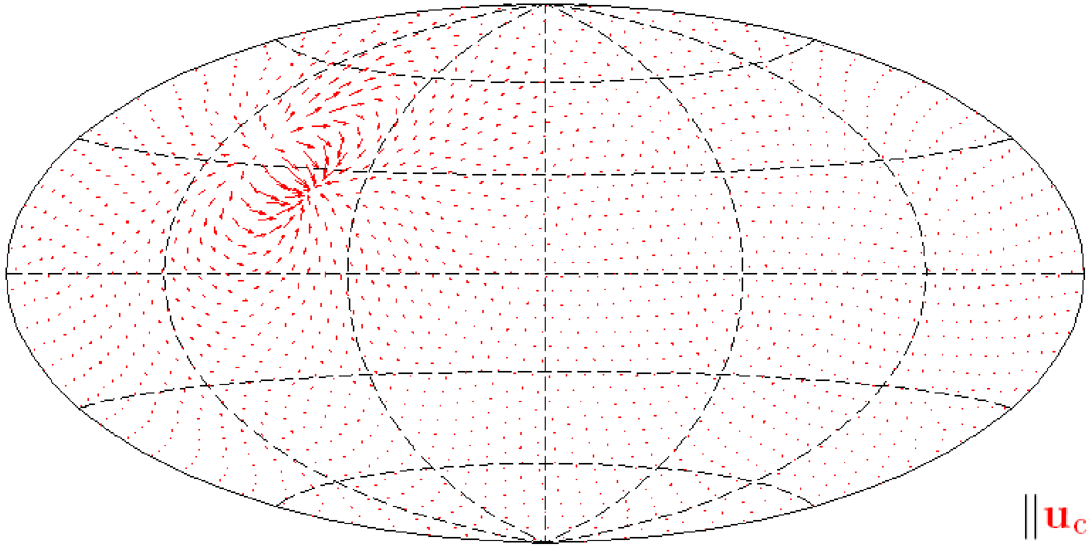

$\|\mathbf{u}_{\text{curl}}\|_2 = 4.3 \text{ m/s}$

Example: decomposition of a geophysical velocity field

- Test case 5 (flow over an isolated mountain) from Williamson *et. al.* JCP (1992).

RBF reconstructed stream function t=15 days

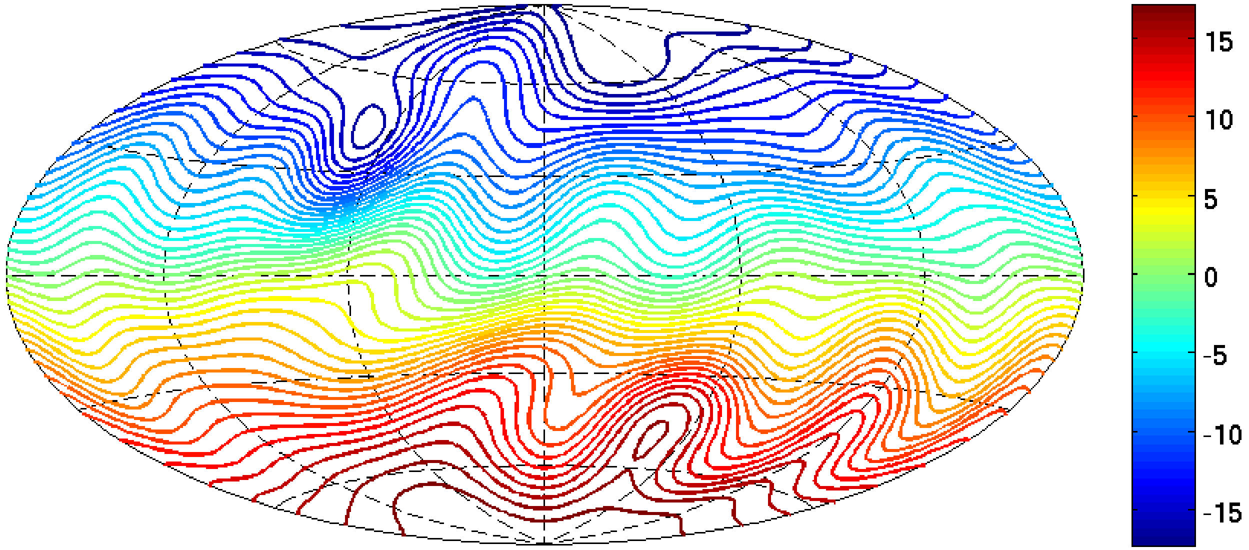

RBF reconstructed velocity potential t=15 days

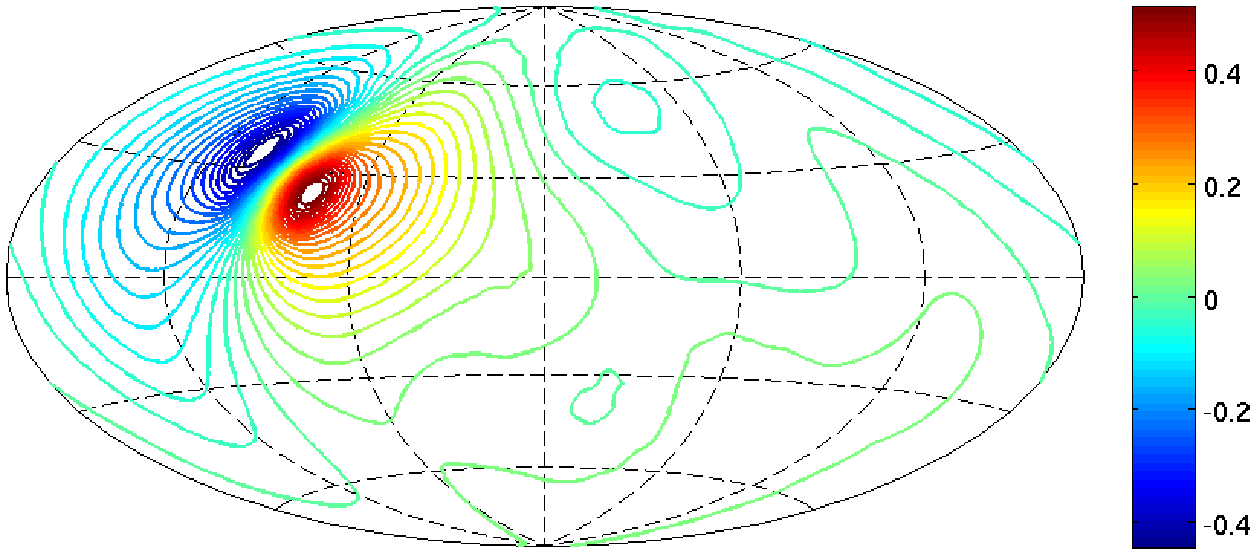

Flow in a rotating differentially heated annulus

- Approximation and decomposition of “real vector fields”.
- Rotating differentially heated annulus for studying the baroclinic instability.

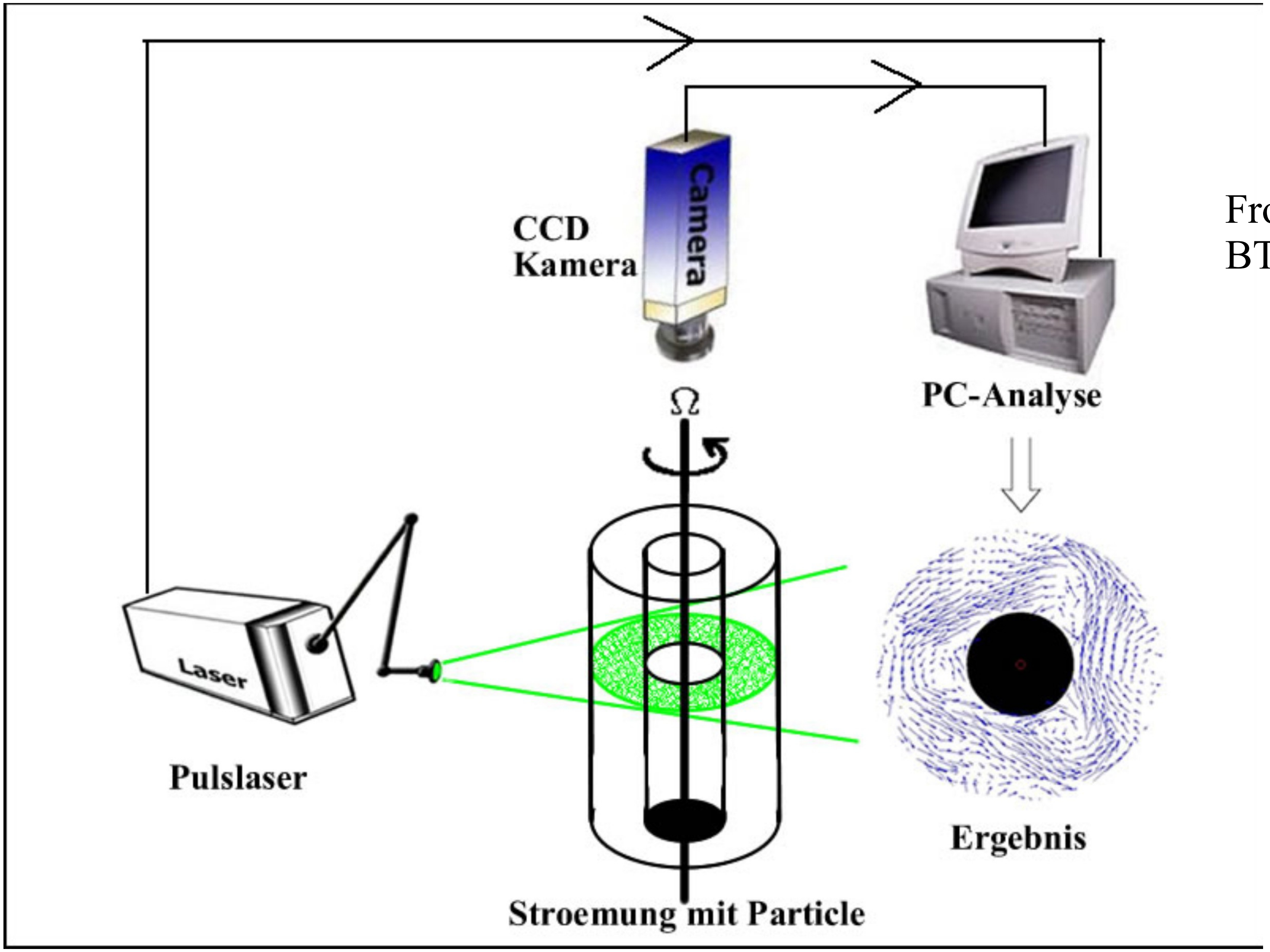

From Harlander,
BTU Cottbus 2008

Joint work with U. Harlander (BTU Cottbus)

Example reconstruction

- Vector field data from PIV measurements at 5 levels in the cylindrical tank:

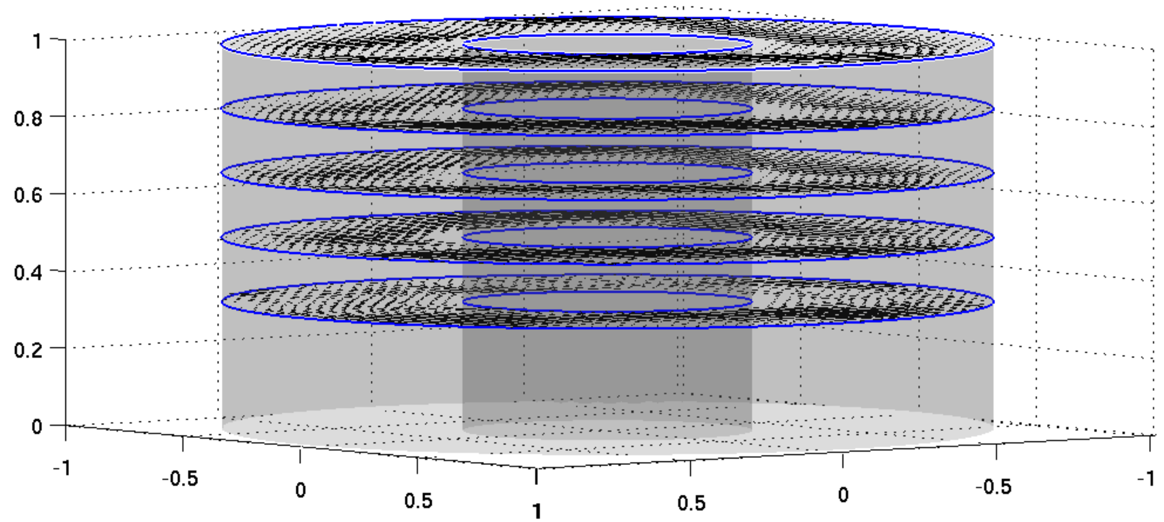

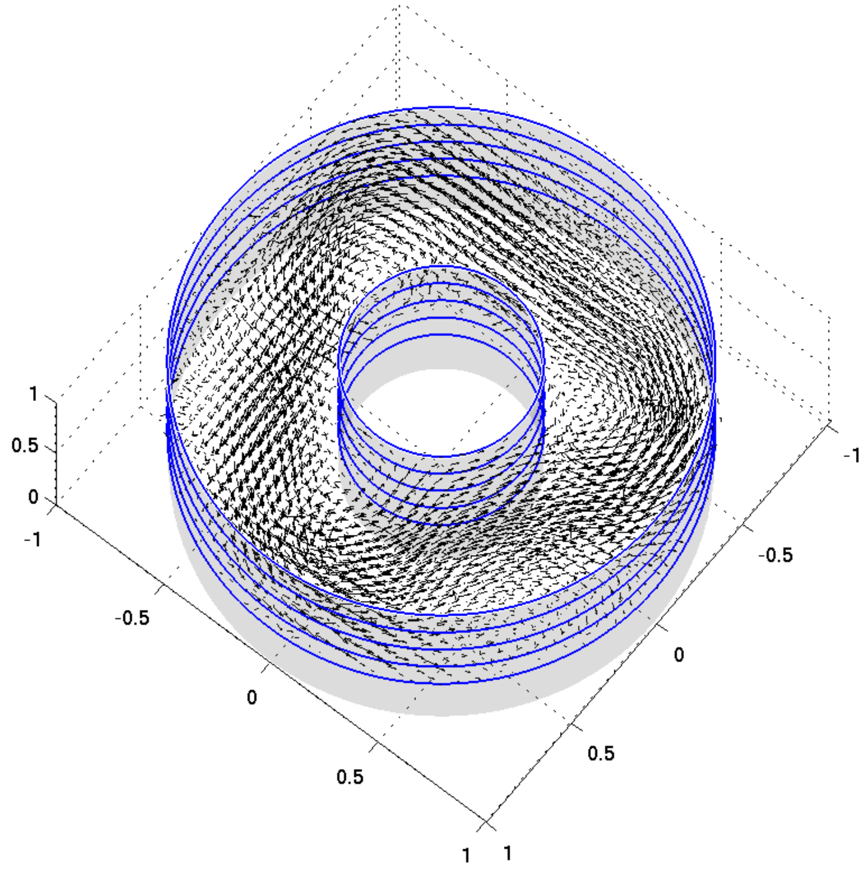

Example reconstruction

- Stream lines of the flow from the RBF reconstructed vector field:

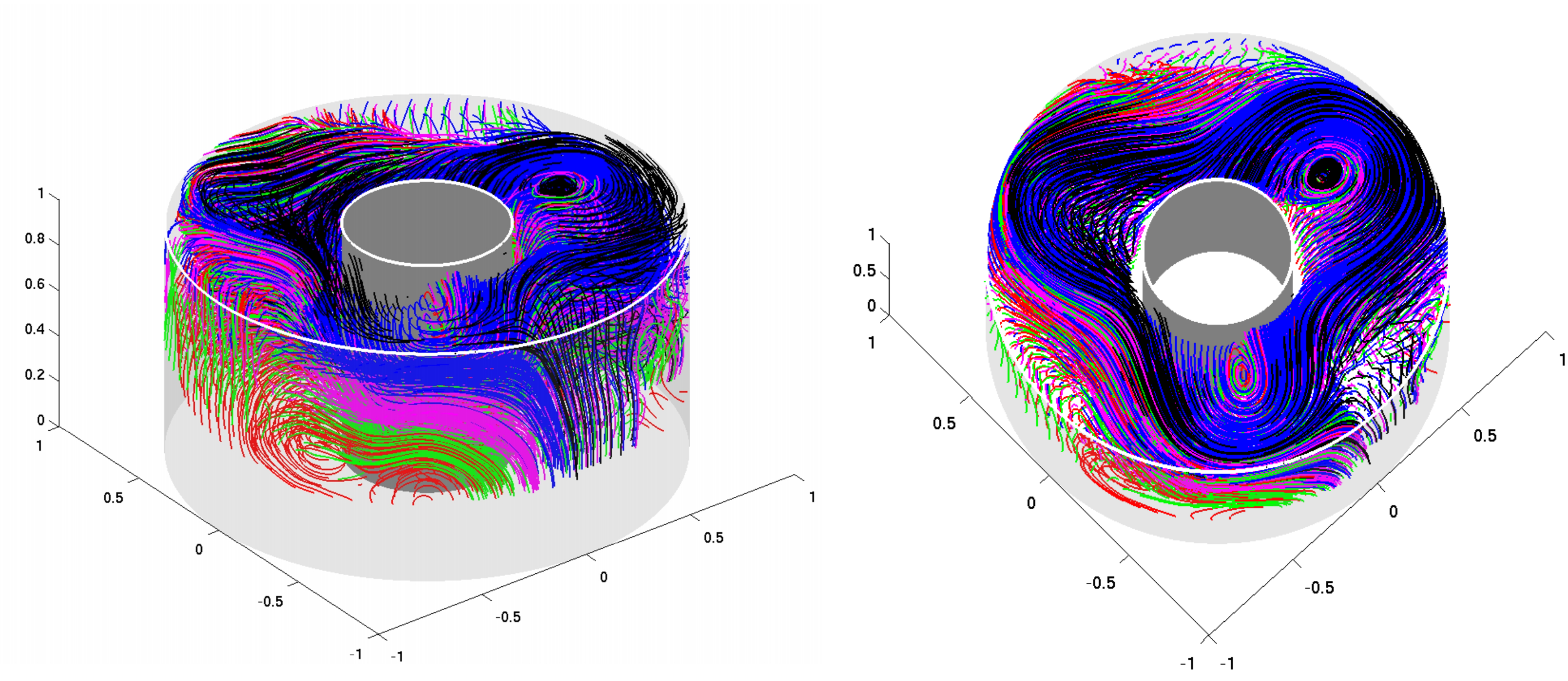

- Colors correspond to traces of particles from different levels in the tank.

This data can be used to validate the numerical simulations of this fluid flow.

Concluding remarks I:

+

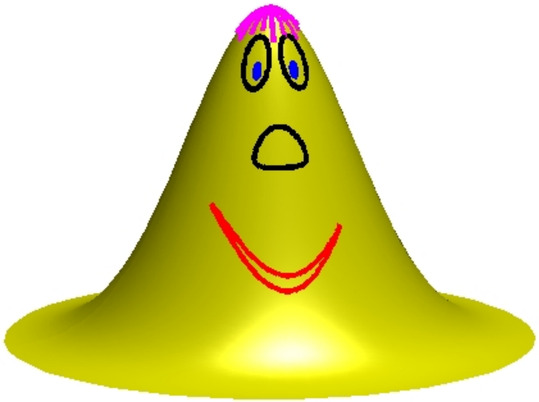

= Significant opportunities

Concluding remarks II:

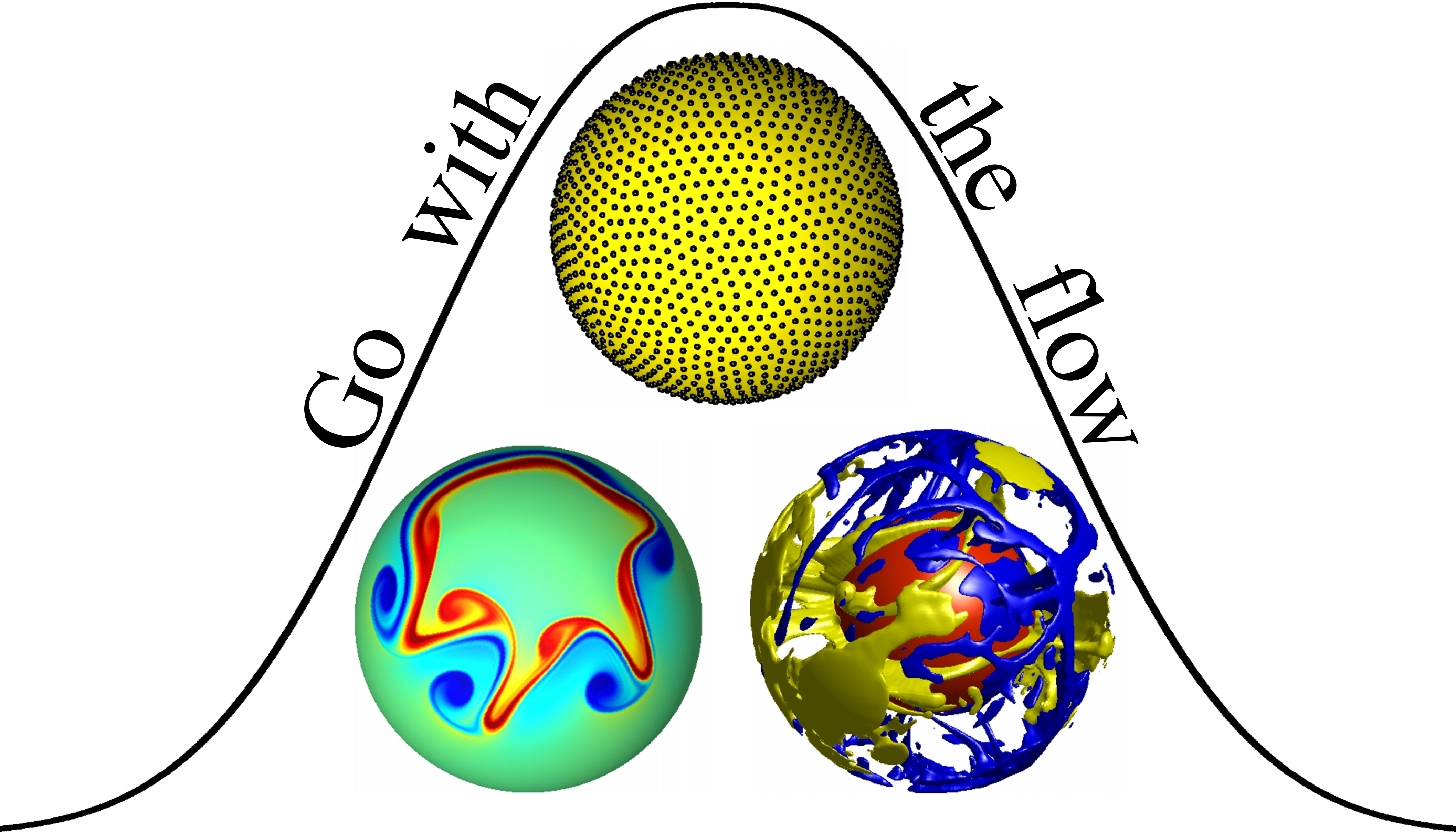

Leave your mesh behind!